

NOTES ON FISSION DYNAMICS

M. Mirea*

Abstract

The dynamics of the nuclear fission is a complex phenomenon, being not yet described adequately from the theoretical point of view. At present, they are not models giving a complete description of the richness of the features which characterizes this phenomenon. It is the main reason for which I called this paper Notes on Fission Dynamics, being certain that I will not be able to make a global description, but only a picture underlining some particularities. So, this mini-overview should be considered only a part of the collection of articles treating the nuclear physics, published as a special number in the review of the Academy of Romanian Scientists, without an exhaustive character. A theory treating the nuclear fission is by excellence based on quantum mechanics. That is, a theory concerning the interactions between the smallest pieces that constitute a many-body nucleus. But, at present it is not possible to perform ab-initio calculations to describe the many-body structure of heavy nuclei which undergo fission by starting from fundamental interactions. To make the problem tractable, the nucleus as a whole are constrained by some collective parameters, associated to some collective degree of freedom. The collective variables are forced to vary, leading to a scission of the nuclear system. The response of the nuclear system to the external forces is given by the nuclear inertia. The mean field potential between the nucleons is obtained after a proper average, and then used to solve the Schrodinger equation. The treatments presented in this article are based on these simplifying concepts. I will give some examples of calculations that include the dissipation and the configuration mixing due to radial and angular couplings. The importance of the subject is also briefly reviewed.

keywords: atomic nucleus, nuclear fission, deformation energy, dissipation energy, nuclear inertia

<https://doi.org/10.56082/annalsarsciophyschem.2020.1.89>

*mirea@nipne.ro Academy of Romanian Scientists, Splaiul Independentei 54, 050094 Bucharest, Romania; Horia Hulubei National Institute for Physics and Nuclear Engineering, P.O. Box MG-6, 077125 Bucharest-Magurele, Romania

1 Introduction

In 1939, the fission was discovered. It is understood as the disintegration process of a atomic nucleus leading to two fragments of comparable masses. From the experimental point of view, the process was evidenced by separating the barium from the products of the uranium bombarded with a neutron beam by Hahn and Strassman. In the same year, Meitner and Frisch gave an explanation for the appearance of these products based on the liquid drop concepts [1, 2]. The fundamental idea can be figured as follows: by overcoming a potential barrier, the initial compound nucleus is split into two smaller droplets, setting free a large amount of energy. Nobody predicted at the time that a neutron can divide a large nucleus into two parts, although for nuclei with masses $A > 120$, the fission process into two nearly equal fragments is exothermic. From this discovery, the fission became an field of research extremely important, in which unsuspected properties of the nucleus were revealed. A lot of phenomenological models were invented to explain the strange experimental findings, but the underlining features are the expressions of quantum mechanics effects. Therefore, the nuclear fission contributed to the development and the validation of the quantum mechanics.

2 Brief history

In their seminal paper published in 1939 [3], Bohr and Wheeler offered a very complex theoretical investigation of the fission process. Their picture is a source for all theoretical descriptions of this phenomenon obtained up to now. In order to explain the fission cross section properties, they assessed that the neutron induced fission cross section is statistically proportional to the number of transition states in the saddle point of a multidimensional barrier, at a given excitation energy. It was also remarked that the fission process is only one possible channel for the disintegration of the compound nucleus, being in competition with the neutron emission and the γ de-excitation. Also, from nuclear densities of states evaluations they showed that the fission cross section is relatively constant up to several MeV. Some neutrons are evaporated at larger excitation energies with some probabilities, and the residual nucleus undergoes fission, determining a multi-chance fission phenomena. Within these essential features, this picture remained unchanged to the present time.

The fission showed a multitude of intriguing aspects and an impressive development of the physics of the fission followed up to 1953 when Hill and Wheeler provided additional key ingredients used to understand theoretically this process [4]. They emphasized that the nucleus is an extremely saturated many body system. Therefore the potential felt by a nucleon in the interior of the nucleus is approximately independent of the positions of the surrounding nucleons. It implies that it is possible to consider the nucleus as a whole, characterizing it with a nuclear shape which can be deformed. Accordingly, the single particle potential is essentially collective,

being managed mainly by its surface boundaries, as a state of the system as a whole. These theoretical assumptions lead to a simplification of the problem, which became tractable with mean field models. Instead to treat the interactions between all nucleons, it becomes convenient to characterize the collective state of a nucleus with the help of some constraints or some generalized coordinates associated to macroscopic degrees of freedom. In this picture, the nucleons move independently in a mean field of a microscopic potential managed by these degrees of freedom. That allows us to construct mean fields by using phenomenological prescriptions [5, 6, 7, 8] or within self-consistent models [9], able to describe properties observed from experiments. The constraints associated to the degrees of freedom are allowed to vary in time leading to the rupture of the initial compound nucleus and leaving to separated fragments. This is essentially our understanding about the fission process.

In neutron induced fission, a direct reaction between the incident bombarding particle and the target can lead to elastic or inelastic scattering, as well as a compound nuclear system. The compound nuclear system disintegrates after a mean life. The simplest treatment is to consider that in the low energy domain, during this short period of time the kinetic energy of the incoming particle is redistributed among the entire nuclear system. For intermediate or high energies, a pre-equilibrium stage should be envisaged, to take into account inelastic processes. The compound nucleus formed when a nucleon hits the internal region of the target nucleus and the cross section of the process is estimated as a solution of the Schrodinger equation for optical model potentials [10, 11, 12]. Once the nucleus is considered as thermalized, the disintegration can be treated within statistical arguments, by calculating the energy widths of the all decay channels. The energy in the fission degree of freedom is always smaller or at most equal to the total excitation of the compound nucleus. For fixed value of total excitation energy, the fission cross section is obtained by summing over the totality of energies in the fission degree of freedom. In other words, a sum of all fission channels is performed within an integration in which the weight is represented by the nuclear density.

In the investigation of the fission process, the more impressive discoveries were empirical in the early stages. Strange experimental findings at the time contributed to the developments of the quantum mechanics, of new concepts in the field. To our days, an exhaustive theoretical approach including the richness and the complexity of the data behavior issued from the experiments is not available. The nuclear structure is still not understood adequately. For example, it is still difficult to reproduce the nuclear masses on the entire nuclear table.

As an example of a strange experimental behavior is the discovery of an isomer in americium [13, 14] together with the presence of intermediate structures in the fission cross sections [15, 16, 17]. These strange behavior were not explained until the postulation of a double humped fission barrier. A such shape of the barrier is impossible to be obtained within the liquid drop model, where a constant distribution of the nuclear density inside the nucleus should be assumed. The deformation

energy should depend on other quantities, as the internal structure of a nucleus. The distortion of the nuclear shape redistributes the single particle states. The rearrangement of the shells translates in modifications of the total deformation energy. These fluctuations, together with the influence of the pairing energy can be taken into account by means of the Strutinsky prescriptions [18, 19, 20]. In the so called macroscopic-microscopic model, oscillatory shell and pairing corrections were added to the smoothly varying liquid drop energy surface. The macroscopic-microscopic energy surface exhibits minima at hyperdeformations, especially where the ratio between the length of the nucleus and its central diameter is about 2, reflecting a stability of shape isomers and the occurrence of deformed closed shells [21, 22].

The experimental mass distributions of fission fragments [23] revealed that the nuclear structure plays a primordial role in the fission process. It was suggested that the asymmetric mass division of fission products is due to a possible preference for $N=82$ magic configuration of the fragments [24]. A first qualitative explanation of the mass-asymmetry of the fission products was given in Ref. [25]. By searching the barrier saddle points of transuranium elements within the Strutinsky prescriptions, it was evidenced that the shapes characterizing the first barrier are reflection symmetric, while those corresponding to second barrier are mass-asymmetric. Regularities in fission mass distribution were exploited in empirical models by relating them to simple mathematical functions [26]. Assuming a statistical equilibrium and involving only three parameters, that is a distance between the complementary fragments, an intrinsic excitation energy, and a collective temperature, correlated with the potential energies of the fragments, the trends of the isotopic yields in the mass and charge distributions, together with their collective kinetic energies were reproduced [27]. Later on, the mass and energy distributions of the fragments were also systematized as function of the primary fragment deformations in three main groups: standard I connected to the spherical shell $N=82$, the standard II connected with $N=88$ and the superlong channels for deformed fragments [28]. By extracting the weights of these fission modes from experimental data, it is possible to improve the evaluations of other quantities that depend on the mass distributions [29], as the neutron multiplicities described by sawtooth distributions.

The mass and charge distributions of the fragments depends on the dynamics of the nuclear system. The fission fragments cannot be formed in their ground states due to energetic restrictions at the scission point, even in the case of adiabatic processes [30, 31]. According to the Bohr-Wheeler model, the fission process can be understood as being realized in two main steps. The first one treats the evolution of the nuclear system up to the top of the outer barrier. A slow adiabatic motion is assumed and the nuclear system behaves as a compound nucleus in thermal equilibrium. The second step consists in a rapid descent from the top of the barrier up to scission, the energy release being converted in internal excitation or translated in collective kinetic energy. The modality in which the energy is shared between the internal degrees of freedom and the macroscopic ones depends on the tensor of

inertia and of the viscosity. As discussed in Ref. [32], the dynamics of the process should explain the broadening of the mass and charge distributions as function of the damping. Two classes of theories are envisaged. The first one provides essentially deterministic solutions by means of the equations of motion in the collective degrees of freedom, the damping being small [33]. The second one considers a strong damping and uses statistical arguments. In a dynamical theory of the first class, the boundary conditions at the saddle point determine uniquely the scission configuration, as obtained in Ref. [33] by means of the Hamilton's equations of motion. If an excitation is considered at the top of the barrier, it follows that a statistical distribution of initial conditions can be envisaged, and the mass distribution is obtained by means of the Liouville theorem. In this formalism, an initial phase-space distribution is connected with a final one. In the statistical theory, an equilibrium between all degrees of freedom is assumed during the descent of the barrier, that is a large dumping hypothesis. A density of states for the nascent fragments at scission can be calculated, being proportional to the mass distribution function. As mentioned in Ref. [32], the two classes of theories become equivalent if an additional dumping can be simulated in the deterministic theories by taking into account mass asymmetry vibrations superimposed on the collective radial motion. These additional vibrations may be obtained by solving the time dependent Schrödinger equation in the mass-asymmetry coordinate as given by the fragmentation theory [34]. Although, it could explain the broadening of the mass distributions, the statistical model was not able to provide information about the dissipation until recently. By exploiting the strong dissipative coupling assumption and by considering the competition between one-body dissipation forces and the cohesive ones, the fragment distributions and the most probable fragment kinetic energies were reproduced [35]. A precise measurement of isotopic distributions of fission products as function of initial excitation energy, by providing information about the kinetic energies, and the angular distributions will contribute to a better understanding of the dynamics of the process. Surprisingly good predictions of mass and kinetic energies distributions were obtained within the Langevin equations of motion [36], recently.

The sawtooth shape of the neutron multiplicity [37, 38, 39] was also explained qualitatively by the asymmetric distribution of fission fragments and the structure of the deformed fission fragments [40, 41]. The neutron multiplicities were used to evaluate the excitation energies as function of the fragment mass [42], evidencing a higher excitation energy for the symmetric fragmentation. This behavior was considered as the evidence of the existence of at least two fission barriers [42, 38]: one for the symmetric fission that leads to excited fragments, and another for the asymmetric fission with moderately excited fragments and high collective kinetic energies. Later on, it was suggested that the neutron emission curves are mainly related to the structure of the deformed final fragments [41] and the excitation due to the dynamics [43]. The neutrons evaporated from fully accelerated fission fragments can be evaluated within statistical prescriptions. A review of the models used for

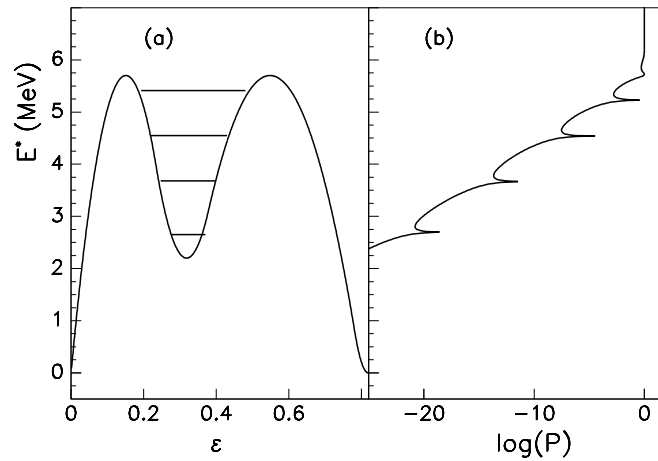


Figure 1: (a) Double fission barrier obtained by means of three smoothed joined parabola plotted as function of a dimensionless elongation variable named ϵ . The parameters of the fission barrier are taken from the work of Ref. [88] and corresponds the compound nucleus ^{238}U . The heights and the minimum of the barrier V are 5.7, 2.2, and 5.7 MeV, with the corresponding stiffnesses $\hbar\omega$ 1, 1 and 0.6 MeV. (b) Dependence between the curve that gives the logarithmic of the penetrability P and the excitation energy E^* of the compound nucleus. The Schrodinger equation was solved within the exact method by extending the formalism of Ref. [75]. The β -resonances in the penetrabilities are connected to the eigenstates constructed in the second potential well displayed in panel (a). The compound resonant states created in the first well are 'filtered' by the resonances of the second well.

such purposes can be found in Ref. [44]. A good agreement with experimental data was obtained in the framework of the Los Alamos model [45] which is based on the knowledge of experimental energy releases. Subsequent developments improved input parameters by means of multiparametric matrices as function of fragment masses, charges and total kinetic energies [46].

A delicate balance between of cohesive nuclear forces on one side, and Coulomb and rotational forces of disruptive character, on the other side, together with fluctuating shell effects and pairing effects gives rise to the deformation energy of the nucleus, that manifests as a surface in the configuration space spanned by the collective variables. For very large angular momentum, the fission barrier may even disappear [47]. Due to the rotational degree of freedom, an anisotropy in the angular distribution of fission fragments is produced, being strongly related on the spin projection K of the transition states on the fission axis. This distribution is a direct consequence of the conservation of the angular momentum, as evidenced in Ref. [48]. For lighter nuclei, it was observed experimentally that the angular distributions exhibit abrupt variations at energies close to the barrier top. These variations were interpreted as a manifestation of the role played by each fission channel. For heavier nuclei, the variation in the angular distribution is attenuated at threshold energies, the manifestation of the structure being attenuated. It was argued [49] that this behavior reveals the presence of an intermediate equilibrium state due to the existence of the isomer minimum. Accordingly, in the case of heavier nuclei, the transition states do not modify so drastically the angular distributions, their external barrier heights being lowered. The presence of an intermediate equilibrium allows the treatments in the frameworks of statistical approaches. A statistical model able to give information about the fragment angular distributions was deduced in Refs. [50, 49, 51, 52]. By using statistical approaches related to the scission configurations, an effective momentum of inertia is assumed constructed as a combination between the parallel and the perpendicular rigid body components. The model provide information about the effective momentum of inertia from the measurement of the mean square value of the fragments angular momenta projections K_0 on the fission axis at the saddle configuration. Therefore some hints concerning the hyperdeformations are guessed. Based on this model, investigations based on experimental data [53] for transuranium elements indicated that the effective momentum of inertia is compatible to the outer barrier deformation at low excitation energies. For high excitation energies, the effective moment of inertia becomes compatible to calculations realized to smaller deformations, that are in accordance to saddle configurations calculated within the liquid drop model. These results show that the shell effects vanish with excitation energies [54] or the order of 50 MeV. For lighter elements, the deformations calculated in this way by using the anisotropy data are in agreement with the liquid drop model expectations. The modifications of the angular distributions for different mass regions were in accordance with theoretical results. For example, a shift of the saddle point position to smaller deformations was predicted with the

two center shell model [55] from the mass region $A=200$ to $A > 230$. In this model, the properties of the fragments manifest in the region of the outer barrier. For mass $A \approx 230$, the fragments shell effects are important, as a influence of the strong shell effects of the doubly magic nucleus ^{132}Sn . It was also suggested that the variation of K_0 at low excitation energy is due to persistence of superfluid effects [56, 57]. It is important to underline that an accurate measurement of the angular distributions can offer valuable information about the nuclear structure at hyperdeformation to test the validity of actual models.

From the previous considerations, it follows that the distributions of the total angular momenta of the primary fission fragments carry information about the whole dynamics and the fission mechanism. The initial angular momentum of the compound nucleus is redistributed not only on the angular momentum of the relative collective motion, but also between intrinsic fragments spins [58]. It was experimentally found that the average spin of the primary fragments in low energy fission is about $7 \hbar$ [59]. However, the fragments spins have rapid fluctuations that depend essentially on the fragment mass and the mass asymmetry of the reaction. Unfortunately, there is currently no consistent theory to predicts the spin distributions in the fragments. A better experimental description will definitely contributes to a development in the theory. As already mentioned, the actual understanding of the angular distributions of fission fragments is based on statistical arguments, by taking into account an effective moment of inertia [50]. This approach was developed by including the dynamics of the fission [60], the latter achievements being described in Ref. [52].

Now, it is established that the fission barrier in the actinide region is characterized by a shape with two or even three maximums [61]. This barrier offers an explanation for the experimental findings, stating with fission isomers, structures in the fission cross section, or angular distributions. Such a barrier is displayed in Fig. 1, approximated with parabolas, as done in general in evaluations. In the region of the threshold excitation energies, that is, close to the maximum of the barrier, the fission cross section reveals a structure formed by a large number of intermediate resonances. These structures are caused by many discrete excited states that exist in the second well of the potential, called class II states. If the fission cross section is calculated as function of the excitation energy, the class II states give rise to resonances in the cross section. To infer the information about the fission shape, it is possible to measure the isomer excitation energy. It is now possible to identify the shape isomers, being obtained by a large variety of nuclear reactions if the energy induced in the system is sufficient to surpass the inner barrier. In this way, some patterns due to the process determined by a neutron inelastic scattering to the isomer, involving also a precision neutron evaporation can be identified in the fission cross section [62]. Also, the rotational bands that are constructed in the second minimum offer information about the hyperdeformed nuclear states. It was found, a verified theoretically within the cranking model, that the rotational

parameter $\hbar^2/(2J)$ is of the order of 3.5 keV, for isomer states. Accordingly, the sub-threshold fission exhibits cluster of resonances, due to the fact that the fission strength is modulated by the class II states. From experimental data, the coupling matrix elements between the class II states and the class I states or about the fission of class II states can be obtained by an analyze of the detailed structure of each cluster. The averaged values of the coupling matrix elements offers directly the order of magnitude of the penetrabilities of the first and second barrier for a given excitation. Also, resonance doublets are identified [63]. They are caused by a degeneracy of the unperturbed class I and class II states. By using a polarized neutron beam, it is possible to assign unambiguously the spin to the detected resonances at low energy [64]. Unfortunately, theoretical predictions of such resonant peaks cannot be realized realistically in terms of actual models, their investigation being concentrated to the activity of analyze.

The scientific community was surprised by many features experimentally detected related to the nuclear fission process. These data developed the theoretical treatments, and step by step, the theory has become increasingly predictive. Therefore, by developing the shell models an island of stability for superheavy nuclei was predicted [65] or and by understanding the fission mechanisms the spontaneous heavy ion emission [66] is assessed from model calculations. In the theory evolution, many new experimental data benchmark the development. The fission still offer new behavior. For a recent example, a new type of asymmetric fission was experimentally observed in the neutron rich ^{180}Hg nucleus [67]. The theory expected that a symmetric distribution of fission fragments should be produced, with an emphasized yield related to the two semi-magic ^{90}Zr products. The explanation that followed in the framework of the macroscopic-microscopic approach improved the actual knowledge by revealing a so-called local minimum in the potential energy surface [68]. The recent developments of this subject are reviewed in Ref. [69]. The bimodal fission phenomena [70] is another recent discovery, in which two components of the kinetic energy spectrum of fission fragments are identified. Moreover, the inversion of the odd-even effect of the low energy fission fragment distributions observed experimentally is difficult to be reproduced theoretically. The odd-odd yields are larger for excitation energies of the fragments lower than 4-5 MeV [71, 72], an effect that can be characterized as strange and that cannot be explained statistically. It was understood by mean of a new dynamical pair breaking effect introduced in the microscopic equations of motion [73].

Despite the improved the theoretical description realized along the time, the fission cross section is still difficult to be reproduced by using microscopic theories, and it is evaluated within phenomenological approaches. For instance, the maximums of the double fission barrier are deduced in an empiric way by using some simple parametrizations for the shape of the barrier and a predefined nuclear level density. As stated many years ago, the cross section is simply proportional with the number of states obtained semi-empirically in the transient point or saddle point

configuration of the barrier following the Bohr-Wheeler hypothesis. The fission cross sections is evaluated always in accordance with some input parameters that rely on experimental observable. For example, at least 6 parameters are needed to reproduce approximately the shape of the fundamental fission barrier. These are, 3 values for the extremes of the potential barrier plus 3 values of the corresponding stiffness parameters of each region of the barrier. In the frame of this approach, it was estimated in Ref. [74] that the fission barrier heights can be extracted with an uncertainty of 0.5-1.0 MeV. Moreover, if the resonant structure of the fission cross section should be reproduced, then the situation is more ambiguous because many transition states are introduced empirically, by hand, to fit the experimental data. So, it can be concluded that this procedure does not include the resonances due to the beta vibrational and to the rotational couplings adequately, in order to understand microscopically the fission process. Therefore, fission of actinides as well as sub-actinides is not yet understood sufficiently for increasing energies above a few MeV. The understanding of the experimental findings still require not only accurate experimental inputs but a sustained effort for their theoretical explanations. At this point, the phenomenological approach that is used in evaluations for the fission cross sections analysis is still limited by many ambiguities and shortcuts. Some of them are mentioned in the following.

In evaluations, the double or triple fission barriers are represented with several smoother joined parabolas [75]. The deviation of the realistic barrier shape from the harmonic one is a cause for an alteration of the values of the penetrabilities. In the approximation used, only at energies close to the fission barrier maximum, confident values of the penetrabilities can be calculated.

An average of the fission cross section is simulated by using a set of values for the heights of the barriers and for the nuclear level density. Unfortunately, it is known that two different sets of values for these quantities can give the same value of the cross section in special circumstances.

The nuclear densities depend on the deformation of the parent nucleus and on its fission trajectory [76]. For the hyperdeformations compatible the region of the outer barrier, the level density is predicted to increase to very large values. One of the reasons is the fact that the moment of inertia is enhanced at hyperdeformations. Therefore the number of transient states is increased. In the evaluations, the variation of the level densities during the fission is treated mainly with phenomenological corrections, some of them in the aim of fitting the data. One of them, the Porter-Thomas distributions [77] are based on statistical analysis of the fluctuations of the reduced widths. Collective vibrational and rotational enhancements of nuclear level densities close to the top of fission barriers in principle can be evaluated microscopically but are also considered in a phenomenological way.

Unfortunately the phenomenological approach is considered as valid for predictions. For example, the heights of the fission barriers obtained from fission data are gathered in systematic and used afterward to predict the cross section of unmeasured

nuclei. In this philosophy, the nuclear structure, that may change dramatically from one nucleus to another, plays a minor role. But, it was seen experimentally that one neutron can change the overall mass distribution from asymmetric to symmetric. A such result is reported in the case of $^{257,258}\text{Fm}$ [78], the existence of at least two competing fission trajectories is postulated.

If a triple fission barrier is postulated, the evaluations show that a dine structure is produced in the fission cross section resonances at the threshold energies, phenomenon generically known as the Th anomaly [79, 80]. A shallow ternary minimum of about 1 MeV was predicted within the macroscopic-microscopic approach at a large amplitude asymmetric shape [81]. As given by the theory, the mass-asymmetry parameter related the third minimum is much more evident than that of the second minimum or that that of the scission point. If the least action principle is used to characterize a fission path it is difficult to fit this behavior. The fission trajectory has to go through different regions of the configuration space to feel the third well. But, a very large increase of the inertia is produced in the inflection point of the trajectory decreasing tremendously the penetrability of the process. Another way to attack the Th anomaly is with dynamical single particle effects [82].

The variation of the nuclear inertia is neglected. It could be incorporated by fitting the widths of the parabolic potential barriers. The stiffness parameters of the parabolas influence the widths of the evaluated cross section resonances. Variation of the nuclear inertia can produce supra-barrier resonances [83]. Moreover, the inertia varies also with the excitation energy [84]. In a realistic treatment, not only the widths of the resonances can be degraded, but their positions are altered.

A nuclear density is a statistical parameter can be calculated only for large values of the excitation energies, where the number of nuclear levels per energy is large. For excitation smaller than several MeV, the excitation spectrum is essentially discrete and can be reproduced with the help of a deformed shell model. But, in the actual calculations even the low energy transition states are evaluated empirically in terms of densities to participate in the fission cross section. However, they are calculations in which some transition states are introduced empirically in the calculations with the aim to reproduce the positions of the experimental fission cross section resonances. These transition states are treated simply as a sequence of levels ordered by their spin that cannot usually intersect during the deformation of the parent nucleus, indexed with different values of the excitation energies in the extreme of the barrier. The number of fitting parameters increases, because for each added excitation the number of input parameters increases with 3, that is, the values of the excitation at the extreme of the barrier. These states are kept in the same ordering, and the existence of the avoided levels crossing region is completely neglected. Especially in the region of the outer barrier, the calculations showed that the density of single particle levels increases, and the probability to produce avoided levels crossings regions is very high. This effect is also reflected by the values of the shell effects, being decreased. It is also known that when a prolate nucleus deforms in its way

to scission, the orbits of the high spin states are preferentially located in a plane perpendicular on the elongation [63]. These orbits are forced to move into a smaller restricted value of the diameter of the nucleus when the nucleus deforms. The single particle energies of the levels with high intrinsic spin should increase. Accordingly, a lot of crossings between levels should be produced during the dynamical evolution, the levels being rearranged. A microscopic calculation should be realized prior to the evaluation in order to identify such level crossings.

The population of the transition states is considered essentially unity. Such assumption is valid only in the case of an adiabatic system, by neglecting residual interactions, as the pairing for example. But, the probability of occupation of a transition state should depend on the dynamics of the process [85]. Due to the rearrangement of the single particle levels, the probabilities of occupation of these states are strongly influenced also by the inherent radial and angular couplings between single particle levels. The probability of occupation increases or decreases as function of the residual interactions, being not compatible to that of an adiabatic system. Accordingly, the population of the transition states should be obtained by solving the microscopic equations of motion.

Due to an incomplete knowledge of the fission mechanism, sometimes a complex fission barrier is used to figure an effective damping, to take into account in a phenomenological way additional de-excitation processes. It is expected that by using an imaginary component of the barrier it is possible to simulate the absorption of the fission degree of freedom into more complicated states caused by additional interactions. As possible processes one can note the γ -deexcitation in the second minimum, or the emission of one pre-scission neutron. However, the description of the coupling between the collective motion and the internal degrees of freedom to infer the dissipation is not possible within this model. By introducing an imaginary component of the barrier in the second well, one obtains two effects: the transmission is reduced and broader resonances are simulated. Unfortunately, the dissipation is not evaluated. Because in the optical model, the fission fragments resort without internal excitation.

In neutron induced fission, a large excitation energy is brought to the compound nucleus. This energy is evaluated in a statistical way, by considering that it is equiprobably shared between intrinsic and external degrees of freedom, as usually considered in the ergodic theory. That is, the collective kinetic energy of the nuclear system can have any value comprised between zero and the maximal amount of the excitation. As mentioned, only one set of parameters characterizes the fission barrier in wide interval of intrinsic excitation energies of the compound nucleus. The cross section fission at a given excitation energy is obtained as a integral over the excitation energy, by spanning with the same probability all the possible values. In these circumstances, for a correct evaluation, the parameters of the fission barrier should be modified when the intrinsic excitation energy increases, due to the disappearance of the shell effects [86]. Always, we are left with a distribution of fission barriers

that depend on the excitation energy. The parameters of the fission barrier should vary in accordance with the intrinsic excitation energy. The actual evaluations cannot include a such phenomenon in calculations, because they need a theoretical calculation of the shell effects at each deformation. The presumed deformation of the parametrized fission barrier is not consistent to a real deformation associated to a degree of freedom obtained from a theoretical model.

The models used in evaluations require the knowledge of the fragments excitation energies. But these information are usually extracted from the experimental data, that is from the quantities that should be theoretically evaluated. The fission cross section data are very complex and carry information about all the interdependent processes, about the nuclear structure, an more important, about effects due to the dynamics of the fragmentation. A very important observable is the dissipation energy obtained at the nuclear rupture. From the theoretical point of view, information about the dissipation can be obtained only from a dynamical treatment of the fission process. But it is difficult to unfold the dynamical effect from the puzzle created by different concurrent mechanisms.

Concerning the evaluations for fission cross sections purposes, it should be reiterated that they depends always on some input parameters extracted from experimental data. So, a vicious circle is created, the evaluated data are based on correlations derived from experimental findings and will not be able to exceed the accuracy with which the findings were obtained [87]. Consequently, the evaluations used in the design of nuclear reactors and other applications demand a high accuracy of experimental data in order to provide confident results. But, in the same time, these evaluations cannot be used confidently to make predictions. Some of the previous ambiguities are know from long time [88, 89, 90], and summarized recently in Ref. [91], but no satisfactory solutions were found. Therefore, if a such analyze is applied to a specific isotope, it provides information about some observable that are only appropriate to the investigated nucleus. The predictions concerning the unmeasured nuclei are questionable due to the lack of consistency. These peculiar aspects can be only solved by investigating microscopically the fission process aiming to provide new information about its basic mechanism [92]. The microscopic approaches used in the fission investigations are subject to many constraints in order to be credible. They should be able to reproduce a large set of experimental data: fission barriers, fission mass distributions, total kinetic energies of fission-fragments, spontaneous lifetimes. It is a huge task. As we will see, theoretical models have yet to be improved to provide data with consistencies comparable to those obtained in fission cross section experiments. For the moment, the best way to solve the enumerated problems is to improve our actual experimental knowledge. The experimental data carry information about all the interdependent mechanism that follow from the structure and the dynamics of fission. Therefore, they should be used as benchmarks for the theoretical investigations.

The prediction degree of the evaluations is strongly related on the accuracy of

the experimental data as well as on the way in which the theoretical achievements are incorporated. Progresses were realized in the statistical modeling of the fission observable corroborating as much as possible information obtained from theoretical concepts [93, 94] or general properties of the nuclear matter. The model predicts the Thomas-Fermi fission barriers in accordance to the topographic theorem [95] by including final shell effects, the individualization of the fission fragments being dictated by the two center shell model behavior [55]. A large spectra of fission observable can be evaluated. Recently, the model was improved by postulating a sorting of the excitation energy at scission [96] modulated by the pairing energy gaps of the fragments. By taking into account the differences in the nuclear densities of the fission partners, final excitations of the order of 3-8 MeV are obtained.

The basic ingredient used in the theoretical study of the large amplitude motion processes is the deformation energy of the nucleus. Apart the phenomenological approaches, macroscopic-microscopic models or Hartree-Fock ones are used to approach the fission process [97, 98]. Within the macroscopic-microscopic method, the measured ground-state energies were reproduced with deviations of 1 MeV [99, 100]. Instead, the values of the fission barrier must be obtained with almost the same uncertainties [101, 102]. The nuclear shapes around scission needs many degrees of freedom to be characterized conveniently [103]. In order to rend the problem tractable, we limit ourselves to a small number of generalized coordinates, that is the elongation, the necking, the deformation of the fragments, the mass-asymmetry, and axial γ -asymmetry. These drawbacks leads to an insufficient description of hyperdeformations, or scission configurations. Moreover, when a parent nucleus undergoes fission, in the scission point, the problem of individualization of the fission fragments is still unsolved. In the scission configuration a unique entangled distribution of microscopic states is calculated. The numbers of proton and of neutron in the two fission fragments are obtained as averages.

In the macroscopic-microscopic approach [104, 105], a parametrization of the independent particle potential should be supplied. There are no arguments to consider this parametrization valid for nuclei far from the line of stability or for hyperdeformations. A more rigorous alternative is to rely on self-consistent potentials given by effective interactions between nucleons which are not related to deformations [106, 107, 108, 109, 110, 111]. In the Hartree-Fock approximation, a smooth self-consistent mean field is obtained because it includes the convolution of many instantaneous densities. If this mean field is varying in time, due to the modifications of some constraints, each single particle wave function is moving independently in the mean field. The Pauli principle is fulfilled. The single particle collision, that must be the cause of the mean field, is incorporated in the equations of motion only in the measure in which they contribute to the mean field potential. Usually, a state dependent pairing model is also used [112]. Unfortunately, the pairing mean field is still considered as function of some parameters as in the density dependent delta interaction approach [113, 114, 115]. The dynamics of the fission process depends strongly

on the parametrization used for the pairing mean field [112, 116]. As mentioned above for the macroscopic-microscopic models, it is questionable if the parametrization is still valid at hyperdeformations. The phenomenological assessed barriers represent a test for the effective interactions. The fission barriers calculated with Hartree-Fock models, using different effective interactions [117, 118, 119, 120, 121] show that the mean field models have become competitive with the macroscopic-microscopic ones.

For large scale collective motion, in general, two approaches are used. On one hand, the generator coordinate method assumes that the internal structure of the evolving systems is equilibrated at each step of the collective motion [122]. On the other hand, the exchange between the collective and intrinsic degrees of freedom is neglected, that is, adiabaticity is assumed [123, 124, 125]. In the low energy domain, when the velocity of the nucleons in the mean field are much greater than the velocities for the modifications of the generalized coordinates, the dynamics problem can be solved using equations of motion or quantum statistics. Up to now, a clear response was not given concerning the modality in which the dissipation energy intervenes in a quantum assembly. In the quantum statistic formalism, it is possible to introduce concepts as friction or viscosity [126], in analogy with the classical mechanics. Concerning the microscopic equations of motion, the problem remains ambiguous. The first step to be overcome is to write down of some time dependent equations for the intrinsic variables. To do that, the variational principle can be used or the Heisenberg form of the equations of motion [127, 128]. In the last kind of treatment, a complete solution that describes the dynamics of the system is obtained. This solution reflects better the response of the nuclear system to the changes of the single particle mean potential. But, there is no clear answer to how to get the dissipation from these results [129]. Dissipation is an irreversible flow of energy and angular momenta from collective degrees of freedom into intrinsic ones. In this sense, both macroscopic-microscopic and Hartree-Fock dynamical models should be improved to be able to reproduce the experimental findings. It should be noticed that uncertainties of only one MeV in the fission barrier heights can be translated in deviations of many order of magnitudes in the calculation of spontaneous fission the half-lives.

The tendency today is to use the Hartree-Fock models. Because, it is assumed that starting from fundamental interactions it will be possible to explain as a whole most of the mysteries surrounding the fission process. The models used in present are able to reproduce only some facets of the richness of the process behavior, and cannot be extended to predict other encountered phenomena.

3 Dynamics

Nuclear reactions were intensively studied in the last thirty years, one of the most intriguing aspects being that the nuclear dynamics is lead in a regime in which the

statistical physics has an important role. Therefore, concepts as friction or thermalization were introduced in this field. Actually, advanced investigations are ongoing to test the basis of these concepts when a small and dense number of fermions are involved, as in the atomic nucleus. The majority of the applications cannot be treated within simple thermodynamic models and require sophisticated concepts of non-equilibrium statistical mechanics, especially to take into consideration of the strong fluctuations. In this sense, as an example we enumerate the fission of ultra hot nuclei and the collisions of heavy ions that lead to very excited nuclei together with multifragmentation. The development of some improved approaches is also motivated by the recent availability of some ion beam facilities ranging almost all the energy domains, from Fermi energies up to relativistic ones. A great part of the theories dealing within these aspects borrowed the idea of non-equilibrium statistic physics, especially the kinetic theory and the stochastic method. These approaches were extended and adapted to the particularities of the nuclear dynamics to treat strong correlated fermions. These theories represent a critical test for the kinetic equations in a strong dissipative regime that implies fluctuations.

In the low energy domain, when the velocity of the nucleons in the mean field are much greater than the velocities for the modifications of the generalized coordinates, the quantum statistic intervene. One behavior observed experimentally is that the fission fragments are usually strongly excited. That is, the process cannot be adiabatic. A flow of energy and angular momentum is produced during the decay, from collective degree of freedom to intrinsic ones. Up to now, a clear response was not given to the modality in which the dissipation energy intervenes in a quantum assembly. The first step to be overcome is to write down of sometime dependent equations for the intrinsic variables. To do that, the variational principle can be used or the Heisenberg form of the equations of motion [127, 128]. In the last kind of treatment, a complete solution that describes the dynamics of the system is obtained. This solution reflects better the response of the nuclear system to the changes of the single particle mean potential. The same solution is obtained within both methods only if the antisymmetric matrix elements of the time derivative operator are neglected. Using this last approximation, it is believed that the major part of the collective energy associated with the coherent motion of the nucleons is eliminated. This part, which is in general neglected, must define the effective mass tensor of the collective motion together with its dependence of the excitation energy.

The dynamics of the nuclear fission was investigated by solving the microscopic equations of motion in Refs. [132, 133, 82, 134, 73, 135, 136, 137, 139, 84, 140] The problem of diabaticity was explored by using a monopole pairing force, sufficiently weak to not strongly redistribute the nucleons so that the mean field does not change significantly. It should be noted that the study available in reference [114] assessed that the seniority state independent pairing force begins to be insufficiently accurate only for nuclei close to the stability lines that characterize the spontaneous emissions

of protons and neutrons in the nuclear map. Close to the stability valley, the BCS approximation used in this project is performing well enough as it can be seen in the global fit of mass realized in reference [130] or in the comparison concerning the density dependent delta interactions in the seniority force in the case of occupation probabilities of single particle levels [131].

In a normal way, the nuclear system is parametrized with several generalized coordinates that parametrize the shape. The independent degrees of freedom are associated to these coordinates. By mean of these generalized coordinates the behavior of all other intrinsic coordinates are determined. The basic ingredient for such an analyze is a nuclear shape parametrization that depends of the degrees of freedom. The generalized variables associated to the degrees of freedom vary in time leading to a compound system and to the split of the nuclear system in two separated fragments. A microscopic potential can be constructed to be consistent within this nuclear shape parametrization. It is known that a nuclear shape can be used for binary processes if the following conditions are satisfied: (I) the three most important degrees of freedom [148], that is elongation, necking and mass asymmetry are taken into consideration; (ii) A sphere and two separated fragments are allowed configurations; (iii) The smoothness of the neck is a independent variable. These three conditions are satisfied by the parametrization used in the following: two ellipsoids with different eccentricities and semi-axis smoothly joined with a median region given by an arc of circle rotated around the axis of symmetry. A good model that can be used in nuclear fission must have at least five degrees of freedom, that is the elongation, the necking, the mass asymmetry and the deformations of the two nascent fragments formed during fission. As our model, this parametrization can characterizes both the configuration associated to a single fragment and that of two separated ones. Also, for this nuclear shape parametrization we will use a two center Woods-Saxon shell model realized by the authors of this proposal. Using this model we are able to solve the mean field potential so that to have only one system of orthogonal wave functions for a two body system that approximate correctly the mean field. Because we have only one system of wave function it is possible to solve correctly the antisymmetrization problem of the total wave function. In the case of one center potentials, the problem of two bodies is solved using molecular methods, using two separated potentials, and the antisymmetry of the total wave function cannot be obtained exactly. Actually, we are the sole group able to use two center Woods-Saxon potentials.

To determine the deformation energy of the system, we use the macroscopic-microscopic method, that is, the total energy is given by the sum of the liquid drop energy and the Strutinski shell and pairing corrections. The liquid drop energy will be computed in the frame of the Yukawa plus exponential model extended for binary systems with different charge densities. The diffusivity electrostatic energy, the Coulomb energy, the surface energy, the volume energy are all included together. To compute the microscopic shell correction we use the single particle diagrams ob-

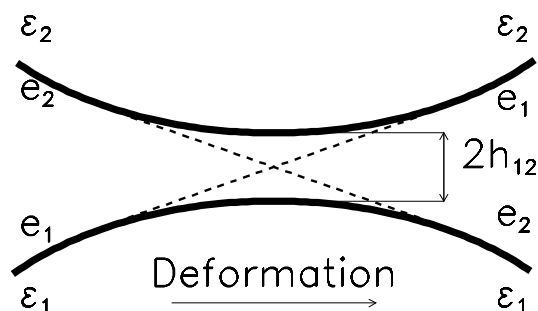


Figure 2: Schematic representation of an avoided levels crossing region. The Landau-Zener effect is produced when a such avoided levels crossing region is produced during the deformation of the nuclear system.

tained within the two center Woods-Saxon shell model. The nuclear inertia will be computed in the frame of the cranking model or in the frame of the gaussian overlap approximation. Once we have a Hamiltonian that contains also the pairing interactions and we introduce the collective parameters through the Lagrange multipliers, the response of the nuclear system for shape changes is obtained with the effective cranking mass. A complex code for this model in the adiabatic hypothesis have been realized recently [135] for the two center Woods Saxon model. Therefore, the two main ingredients too calculate the action are at our disposal.

The shape of the potential barrier can be obtained only if the trajectory of the nuclear system in the configuration space spanned by the five generalized coordinates associated to the degrees of freedom is known. This trajectory is obtained by the minimization of the action integral or by solving the Euler Lagrange equations of motion. Up to now, the minimization methods were realized only for adiabatic systems. We will introduce in the frame of the method the calculation of the dissipated energy within the time dependent pairing equations, that are similar to Hartree-Fock-Bogoliubov equations of motion. These equations are deduced from the variational method. The variation versus the time of the Bogoliubov wave function amplitudes in seniority 0, 1 or 2 states are obtained. The equations of motion for the mixing between seniority 1 configurations will be deduced by incorporating the Landau-Zener dynamical effect and the Coriolis couplings, as generalized recently [141, 73].

3.1 The microscopic equations of motion for seniority-1 mixing

Two microscopic effects participate to the mixing of the configurations during the large amplitude motion: the Landau-Zener promotion mechanism [142, 143, 144] and the Coriolis coupling [145]. Two levels with the same good quantum numbers associated to some symmetries of the nuclear system cannot intersect during the

deformation and exhibit avoided levels crossings regions. In Fig. 2, a such avoided levels crossing region is schematically represented. In such a region, the adiabatic levels ϵ_1 and ϵ_2 exchange their characteristics. If a nucleon is located initially on the adiabatic level ϵ_1 , and the passage of the avoided levels crossing region is made slowly, the nucleon will remain on the same adiabatic state ϵ_1 with a great probability. If the passage is made rapidly, with a large deformation velocity, the the nucleon will skip with a great probability on the superior adiabatic level ϵ_2 . In this case, the nucleon follows the diabatic state e_1 . The interaction energy between the diabatic states e_1 and e_2 is given by the energy difference at the distance of closed approach between the two single particle levels, that is $2h_{12}$.

In this section, as an example, the equations of motion for the seniority-1 nuclear systems are deduced. These differential equations takes into account the microscopic effects that cause the configuration mixing. In the framework of the variational principle, one has to minimize the functional

$$\delta\mathcal{L} = \delta \langle \varphi_{IM} | H + H_R - i\hbar \frac{\partial}{\partial t} + H' - \lambda | N_2 \hat{N}_1 - N_1 \hat{N}_2 | \varphi_{IM} \rangle \quad (1.1)$$

where H is the many-body Hamiltonian which includes the pairing l interaction, H_R is the centrifugal energy, H' is the term which allows the Landau-Zener effect [141], while \hat{N}_1 and \hat{N}_2 are particles numbers operators acting on the two fragments that are formed in the scission region. The condition introduced in term of particle number operators determines a dynamical projection of the numbers of particles on the two final fragments [139]. Here, λ is a Lagrange multiplier. In the energy functional (1.1), the trial many body wave function is given as a superposition of seniority-1 Bogoliubov wave functions, allowing rotations. The trial wave function is defined as follows:

$$|\varphi_{IM}\rangle = \sum_{\Omega, m} c_{\Omega, m} b_{I, M, \Omega, m}^+ \prod_{(\Omega', l) \neq (\Omega, m)} \left(u_{\Omega', l(\Omega, m)} + v_{\Omega', l(\Omega, m)} a_{\Omega', l}^+ a_{\Omega', l} \right) |0\rangle \quad (1.2)$$

where $c_{\Omega, mm}$ are amplitudes. The square of these amplitudes supply the probability to obtain a given configuration. The creation and annihilation operators for the single particle state (Ω, l) are $a_{\Omega, l}^+$ and $a_{\Omega, l}$, respectively. The BCS occupation and vacancy amplitudes are $v_{\Omega, l}$ and $u_{\Omega, l}$, respectively. With

$$\bar{\Omega} = -|\Omega| \quad (1.3)$$

are denoted the intrinsic spin projections on the axis of symmetry. With

$$b_{IM\Omega n}^+ |0\rangle = \left(\frac{2I+1}{8\pi^2} \right)^{1/2} \left(\frac{\Omega}{|\Omega|} \right)^{I+\Omega} \mathcal{D}_{M\Omega}^I(\omega) a_{\Omega n}^+ |0\rangle \quad (1.4)$$

one denoted a product between the creation operator $a_{\Omega, m}^+$ of the blocked level and the rotation function $\mathcal{D}_{M\Omega}^I(\omega)$. The relevant properties of the rotation function are

$$I_{\pm} \mathcal{D}_{M\Omega}^I(\omega) = [(I \pm \Omega)(I \mp \Omega + 1)]^{1/2} \mathcal{D}_{M\Omega \mp 1}^I(\omega), \quad (1.5)$$

$$I^2 \mathcal{D}_{M\Omega}^I(\omega) = I(I+1) \mathcal{D}_{M\Omega}^I(\omega), \quad (1.6)$$

$$\langle IM\Omega \mp 1 | I_{\pm} | IM\Omega \rangle = ((I \pm \Omega)(I \mp \Omega + 1))^{1/2}, \quad (1.7)$$

being useful in the calculation of matrix elements.

To deduce the equations of motion, first of all, the elements of the Hamiltonian should be obtained. For the single particle energies, after some algebra one obtains the next formula:

$$\begin{aligned} \langle a_k^+ \prod_{l \neq k} (u_l + v_l a_l^+ a_l^+) | \sum_k \epsilon_k (a_k^+ a_k + a_{\bar{k}}^+ a_{\bar{k}}) | a_k^+ \prod_{l \neq k} (u_l + v_l a_l^+ a_l^+) \rangle & \quad (1.8) \\ & = 2 \sum_{l \neq k} \rho_l \epsilon_l + \epsilon_k. \end{aligned}$$

where ϵ_l are single particle energies. The single particle densities $\rho_l = |v_l|^2$ and the pairing moment components $\kappa_l = u_l v_l$ are used in the final expressions. For the pairing rezidual interactions, one finds:

$$\begin{aligned} \langle a_k^+ \prod_{l \neq k} (u_l + v_l a_l^+ a_l^+) | G \sum_n a_n^+ a_n^+ a_{\bar{l}} a_l | a_k^+ \prod_{l \neq k} (u_l + v_l a_l^+ a_l^+) \rangle & \quad (1.9) \\ = -\frac{|\Delta_k|^2}{G} - G \sum_{l \neq k} \rho_l^2 \end{aligned}$$

where $\Delta_k = G \sum u_k v_k$ is known as the pairing gap parameter. For the condition of normalization one obtains:

$$\begin{aligned} \langle a_k^+ \prod_{l \neq k} (u_l + v_l a_l^+ a_l^+) | \lambda \hat{N} | a_k^+ \prod_{l \neq k} (u_l + v_l a_l^+ a_l^+) \rangle & \quad (1.10) \\ = 2 \sum_l \lambda \rho_l + 1. \end{aligned}$$

One needs also to calculated the matrix elements of the expressions obtained with the angular momentum ladder operators.

$$\begin{aligned} \langle \varphi' | j_{\pm} | \varphi \rangle & = \sum_{m'm} c_{m'}^* c_m \langle 0 | a_{m'} \prod_{l' \neq m'} (u_{l'(m')} + v_{l'(m')}^* a_{l'} a_{\bar{l}'}) j_{\pm} \\ & \quad \times \left[a_m^+ \prod_{l \neq m} (u_{l(m)} + v_{l(m)} a_l^+ a_l^+) \right] | 0 \rangle \end{aligned} \quad (1.11)$$

To effectuate this calculation, one identifies two cases. The first situation is for $m' = m$, that is the matrix elements between the same seniority-1 configuration. That gives:

$$\begin{aligned} & \sum_m |c_m|^2 \langle 0 | a_m \prod_{l \neq m} (u_{l(m)} + v_{l(m)}^* a_l a_{\bar{l}}) j_{\pm} \left[a_m^+ \prod_{l \neq m} (u_{l(m)} + v_{l(m)} a_l^+ a_l^+) \right] | 0 \rangle \\ & = \sum_m |c_m|^2 \langle 0 | a_m \prod_{l \neq m} (u_{l(m)} + v_{l(m)}^* a_l a_{\bar{l}}) \left[(j_{\pm} a_m^+) \prod_{l \neq m} (u_{l(m)} + v_{l(m)} a_l^+ a_l^+) \right. \\ & \quad \left. + a_m^+ \sum_n (u_{n(m)} j_{\pm} + v_{n(m)} \{ (j_{\pm} a_n^+) a_n^+ + a_n^+ (j_{\pm} a_n^+) \}) \right] | 0 \rangle \\ & \quad \times \prod_{l \neq m, n} (u_{l(m)} + v_{l(m)} a_l^+ a_l^+) | 0 \rangle \end{aligned} \quad (1.12)$$

All the previous terms should be zero. The second case is when the matrix element $\langle 0|a_{m'}J_{\pm}a_m^{\pm}|0\rangle$ is different from zero. The next equations are obtained

$$\begin{aligned}
& \sum_{m',m} c_{m'}^* c_m \left\langle 0 \left| a_{m'} \prod_{l' \neq m'} \left(u_{l'(m')} + v_{l'(m')}^* a_{l'} a_{\bar{l}'} \right) j_{\pm} \right. \right. \\
& \quad \times \left. \left. \left[a_m^{\pm} \prod_{l \neq m} \left(u_{l(m)} + v_{l(m)} a_l^{\pm} a_{\bar{l}}^{\pm} \right) \right] \right| 0 \right\rangle \\
& = \sum_{m',m} c_{m'}^* c_m \left\langle 0 \left| a_{m'} \prod_{l' \neq m'} \left(u_{l'(m')} + v_{l'(m')}^* a_{l'} a_{\bar{l}'} \right) \right. \right. \\
& \quad \times \left. \left. \left[(j_{\pm} a_m^{\pm}) \prod_{l \neq m} \left(u_{l(m)} + v_{l(m)} a_l^{\pm} a_{\bar{l}}^{\pm} \right) \right. \right. \right. \\
& \quad \left. \left. \left. + a_m^{\pm} \sum_n \left(u_{n(m)} j_{\pm} + v_{n(m)} \{ (j_{\pm} a_n^{\pm}) a_n^{\pm} + a_n^{\pm} (j_{\pm} a_n^{\pm}) \} \right) \right. \right. \right. \\
& \quad \left. \left. \left. \times \prod_{l \neq m, n} \left(u_{l(m)} + v_{l(m)} a_l^{\pm} a_{\bar{l}}^{\pm} \right) \right] \right| 0 \right\rangle
\end{aligned} \tag{1.13}$$

The first term in the right hand side can be readily transformed as

$$\begin{aligned}
& \sum_{m',m} c_{m'}^* c_m \left\langle 0 \left| a_{m'} \prod_{l' \neq m'} \left(u_{l'(m')} + v_{l'(m')}^* a_{l'} a_{\bar{l}'} \right) \right. \right. \\
& \quad \times \left. \left. (j_{\pm} a_m^{\pm}) \prod_{l \neq m} \left(u_{l(m)} + v_{l(m)} a_l^{\pm} a_{\bar{l}}^{\pm} \right) \right| 0 \right\rangle \\
& = \sum_{m',m} c_{m'}^* c_m \left\langle 0 \left| a_{m'} \left(u_{m(m')} + v_{m(m')}^* a_m a_{\bar{m}} \right) \right. \right. \\
& \quad \times \left. \left. (j_{\pm} a_m^{\pm}) \left(u_{m'(m)} + v_{m'(m)} a_{m'}^{\pm} a_{\bar{m}'}^{\pm} \right) \right| 0 \right\rangle \\
& = \sum_{m',m} c_{m'}^* c_m (u_{m(m')} u_{m'(m)}) \langle 0 | a_{m'} j_{\pm} a_m^{\pm} | 0 \rangle
\end{aligned} \tag{1.14}$$

By indexing with Ω and m the result is:

$$\begin{aligned}
& \sum_{m',m} c_{m'}^* c_m (u_{m(m')} u_{m'(m)}) \langle 0 | a_{m'} j_{\pm} a_m^{\pm} | 0 \rangle \\
& = \sum_{\Omega, m', m} c_{\Omega \pm 1, m'}^* c_{\Omega, m} (u_{\Omega, m(\Omega \pm 1, m')} u_{\Omega \pm 1, m'(\Omega, m)}) \langle 0 | a_{\Omega \pm 1, m'} j_{\pm} a_{\Omega, m}^{\pm} | 0 \rangle
\end{aligned} \tag{1.15}$$

For $n = m'$, the second term in the right hand side gives:

$$\begin{aligned}
& \sum_{m',m} c_{m'}^* c_m \left\langle 0 \left| a_{m'} \prod_{l' \neq m'} \left(u_{l'(m')} + v_{l'(m')}^* a_{l'} a_{\bar{l}'} \right) a_m^{\pm} \right. \right. \\
& \quad \times \sum_n \left(u_{n(m)} + v_{n(m)} \{ (j_{\pm} a_n^{\pm}) a_n^{\pm} + a_n^{\pm} (j_{\pm} a_n^{\pm}) \} \right) \\
& \quad \left. \prod_{l \neq m, n} \left(u_{l(m)} + v_{l(m)} a_l^{\pm} a_{\bar{l}}^{\pm} \right) \right| 0 \right\rangle \\
& = \sum_{m',m} c_{m'}^* c_m \left\langle 0 \left| a_{m'} \left(u_{m(m')} + v_{m(m')}^* a_m a_{\bar{m}} \right) \right. \right. \\
& \quad \times \left. \left. a_m^{\pm} \left(u_{m'(m)} + v_{m'(m)} \{ (j_{\pm} a_{m'}^{\pm}) a_{\bar{m}'}^{\pm} + a_{m'}^{\pm} (j_{\pm} a_{m'}^{\pm}) \} \right) \right| 0 \right\rangle \\
& = \sum_{m',m} c_{m'}^* c_m \left\langle 0 \left| v_{m(m')}^* v_{m'(m)} a_{m'} a_m a_{\bar{m}} a_m^{\pm} \left[(j_{\pm} a_{m'}^{\pm}) a_{\bar{m}'}^{\pm} + a_{m'}^{\pm} (j_{\pm} a_{m'}^{\pm}) \right] \right| 0 \right\rangle \\
& = \sum_{m',m} c_{m'}^* c_m \left\langle 0 \left| v_{m(m')}^* v_{m'(m)} a_{\bar{m}} j_{\pm} a_{m'}^{\pm} \right| 0 \right\rangle
\end{aligned} \tag{1.16}$$

By indexing with Ω and m , this term becomes:

$$\begin{aligned}
& \sum_{m',m} c_{m'}^* c_m \left\langle 0 \left| v_{m(m')}^* v_{m'(m)} a_{\bar{m}} j_{\pm} a_{m'}^{\pm} \right| 0 \right\rangle \\
& = \sum_{\Omega, m', m} c_{\Omega \pm 1, m'}^* c_{\Omega, m} (v_{\Omega, m(\Omega \pm 1, m')}^* v_{\Omega \pm 1, m'(\Omega, m)}) \langle 0 | a_{\Omega \pm 1, m'} j_{\pm} a_{\Omega, m}^{\pm} | 0 \rangle
\end{aligned} \tag{1.17}$$

The final results is:

$$\begin{aligned}
\langle \varphi' | j_{\pm} | \varphi \rangle &= \sum_{m',m} c_{m'}^* c_m [(u_{m(m')} u_{m'(m)}) \langle 0 | a_{m'} j_{\pm} a_m^+ | 0 \rangle \\
&+ (v_{m(m')}^* v_{m'(m)}) \langle 0 | a_{\bar{m}} j_{\pm} a_{\bar{m}'}^+ | 0 \rangle] \\
&= \sum_{m',m} c_{m'}^* c_m (u_{m(m')} u_{m'(m)} + v_{m(m')}^* v_{m'(m)}) \langle 0 | a_{m'} j_{\pm} a_m^+ | 0 \rangle
\end{aligned} \tag{1.18}$$

That is, indexing with Ω and m , the matrix elements are

$$\begin{aligned}
&\sum_{m',m} c_{m'}^* c_m (u_{m(m')} u_{m'(m)} + v_{m(m')}^* v_{m'(m)}) \langle 0 | a_{m'} j_{\pm} a_m^+ | 0 \rangle \\
&= \sum_{\Omega, m', m} c_{\Omega \pm 1, m'}^* c_{\Omega, m} (u_{\Omega, m(\Omega \pm 1, m')} u_{\Omega \pm 1, m'(\Omega, m)} + v_{\Omega, m(\Omega \pm 1, m')}^* v_{\Omega \pm 1, m'(\Omega, m)}) \\
&\langle 0 | a_{\Omega \pm 1, m'} j_{\pm} a_{\Omega, m}^+ | 0 \rangle
\end{aligned} \tag{1.19}$$

The matrix elements within the rotation functions are given by the next expression:

$$\begin{aligned}
\langle \varphi'_{IM} | I_{\mp} j_{\pm} | \varphi_{IM} \rangle &= \sum_{\Omega', \Omega, m', m} c_{\Omega', m'}^* c_{\Omega, m} \\
&\left[(u_{\Omega, m(\Omega', m')} u_{\Omega', m'(\Omega, m)}) \langle \mathcal{D}_{M\Omega'}^I | I_{\mp} | \mathcal{D}_{M\Omega}^I \rangle \langle 0 | a_{\Omega', m'} j_{\pm} a_{\Omega, m}^+ | 0 \rangle \right. \\
&\left. + (v_{\Omega, m(\Omega', m')}^* v_{\Omega', m'(\Omega, m)}) \langle \mathcal{D}_{M\bar{\Omega}'}^I | I_{\mp} | \mathcal{D}_{M\bar{\Omega}}^I \rangle \langle 0 | a_{\bar{\Omega}, m} j_{\pm} a_{\bar{\Omega}', m'}^+ | 0 \rangle \right].
\end{aligned} \tag{1.20}$$

The rotational energy for the axial symmetric rotor is defined as:

$$H_R = \frac{\hbar^2}{2J} (I^2 - j_3^2) + \frac{\hbar^2}{2J} (j_1^2 + j_2^2) - \frac{\hbar^2}{2J} (j_+ I_- + j_- I_+) \tag{1.21}$$

Therefore, the matrix elements to be calculated are:

$$\begin{aligned}
&\langle \varphi'_{IM} | j_+ I_- + j_- I_+ | \varphi_{IM} \rangle \\
&= \sum_{\Omega=-I, I} \sum_{n', n} c_{\Omega+1, n'}^* c_{\Omega, n} ((I - \Omega)(I + \Omega + 1))^{1/2} \\
&\times \left[u_{\Omega, n(\Omega+1, n')} u_{\Omega+1, n'(\Omega, n)} + v_{\Omega, n(\Omega+1, n')}^* v_{\Omega+1, n'(\Omega, n)} \right] \\
&\times \langle a_{\Omega+1, n'}^+ | j_+ | a_{\Omega, n}^+ \rangle \\
&+ \sum_{\Omega=-I, I} \sum_{n', n} c_{\Omega-1, n'}^* c_{\Omega, n} ((I + \Omega)(I - \Omega + 1))^{1/2} \\
&\times \left[u_{\Omega, n(\Omega-1, n')} u_{\Omega-1, n'(\Omega, n)} + v_{\Omega, n(\Omega-1, n')}^* v_{\Omega-1, n'(\Omega, n)} \right] \\
&\times \langle a_{\Omega-1, n'}^+ | j_- | a_{\Omega, n}^+ \rangle
\end{aligned} \tag{1.22}$$

for $\Omega = -I, \dots, I$. It is also important to determine the next expressions:

$$\begin{aligned}
\langle \varphi' | j_x^2 | \varphi \rangle &= \sum_{\Omega, n} \left\langle \varphi' | j_x | a_{\Omega, n}^+ \prod_{(\Omega', n') \neq (\Omega, n)} (u_{\Omega', n'(\Omega, n)} + v_{\Omega', n'(\Omega, n)} a_{\Omega', n'}^+ a_{\bar{\Omega}', n'}^+) \right\rangle \\
&\left\langle a_{\Omega, n}^+ \prod_{(\Omega', n') \neq (\Omega, n)} (u_{\Omega', n'(\Omega, n)} + v_{\Omega', n'(\Omega, n)} a_{\Omega', n'}^+ a_{\bar{\Omega}', n'}^+) | j_x | \varphi \right\rangle
\end{aligned} \tag{1.23}$$

where the angular momenta $j_x = (j_+ + j_-)/2$ and $j_y = (j_+ - j_-)/2i$ are given in terms of ladder operators. That means also that when the term j^2 is evaluated, the terms of the type $j_+ \times j_-$ are positive for j_y^2 . In the same time, the terms of the

type $j_+ \times j_+$, $j_- \times j_-$ will be canceled with terms obtained from j_x^2 . The first step is to calculate

$$\begin{aligned} \langle \varphi_{m'} | j_+ + j_- | \varphi_m \rangle &= \langle 0 | a_{m'} \prod_{l' \neq m'} (u_{l'}(m') + v_{l'}^*(m') a_{l'} a_{l'}^\dagger) \\ &\times (j_+ + j_-) a_m \prod_{l \neq m} (u_l(m) + v_l(m) a_l^\dagger a_l^\dagger) | 0 \rangle \end{aligned} \quad (1.24)$$

Here, one has many possibilities: $m' = m$ where the integral is zero; $m' \neq m$ where the integral is zero with only one exception $m' = l$ and $l' = m$. In this last case, one obtains

$$\begin{aligned} \langle \varphi_{m'} | j_+ + j_- | \varphi_m \rangle &= \langle 0 | a_l (u_{m(l)} + v_{m(l)}^* a_m a_m^\dagger) (j_+ + j_-) a_m (u_l(m) + v_l(m) a_l^\dagger a_l^\dagger) | 0 \rangle \\ &= u_{m(l)} u_l(m) \langle 0 | a_l (j_+ + j_-) a_m^\dagger | 0 \rangle + v_{m(l)}^* v_l(m) \langle 0 | a_m (j_+ + j_-) a_l^\dagger | 0 \rangle \end{aligned} \quad (1.25)$$

Therefore, it follows:

$$\begin{aligned} &\sum_m \langle \varphi_l | j_+ + j_- | m \rangle \langle m | j_+ + j_- | \varphi_{l'} \rangle \\ &= \sum_m c_l^* c_{l'} \left[u_{m(l)} u_l(m) \langle a_l^\dagger | j_+ + j_- | a_m^\dagger \rangle + v_{m(l)}^* v_l(m) \langle a_m^\dagger | j_+ + j_- | a_l^\dagger \rangle \right] \\ &\times \left[u_{l'(m)} u_{m(l')} \langle a_{l'}^\dagger | j_+ + j_- | a_{l'}^\dagger \rangle + v_{l'(m)}^* v_{m(l')} \langle a_{l'}^\dagger | j_+ + j_- | a_m^\dagger \rangle \right] \\ &= \sum_m c_l^* c_{l'} \left[u_{m(l)} u_l(m) u_{l'(m)} u_{m(l')} \langle a_l^\dagger | j_+ + j_- | a_m^\dagger \rangle \langle a_m^\dagger | j_+ + j_- | a_{l'}^\dagger \rangle \right. \\ &+ u_{m(l)} u_l(m) v_{l'(m)}^* v_{m(l')} \langle a_l^\dagger | j_+ + j_- | a_m^\dagger \rangle \langle a_{l'}^\dagger | j_+ + j_- | a_m^\dagger \rangle \\ &+ v_{m(l)}^* v_l(m) u_{l'(m)} u_{m(l')} \langle a_m^\dagger | j_+ + j_- | a_l^\dagger \rangle \langle a_m^\dagger | j_+ + j_- | a_{l'}^\dagger \rangle \\ &\left. + v_{m(l)}^* v_l(m) v_{l'(m)}^* v_{m(l')} \langle a_m^\dagger | j_+ + j_- | a_l^\dagger \rangle \langle a_{l'}^\dagger | j_+ + j_- | a_m^\dagger \rangle \right] \end{aligned} \quad (1.26)$$

Because $\langle a_m^\dagger | j_+ + j_- | a_l^\dagger \rangle = \langle a_l^\dagger | j_+ + j_- | a_m^\dagger \rangle$, then it is straightforward to deduce

$$\begin{aligned} &\sum_m \langle \varphi_l | j_+ + j_- | m \rangle \langle m | j_+ + j_- | \varphi_{l'} \rangle \\ &= \sum_m c_l^* c_{l'} \left(u_{m(l)} u_l(m) + v_{m(l)}^* v_l(m) \right) \langle a_l^\dagger | j_+ + j_- | a_m^\dagger \rangle \\ &\times \left(u_{l'(m)} u_{m(l')} + v_{l'(m)}^* v_{m(l')} \right) \langle a_m^\dagger | j_+ + j_- | a_{l'}^\dagger \rangle + \\ &= \sum_m c_l^* c_{l'} \left[u_{m(l)} u_l(m) u_{l'(m)} u_{m(l')} \langle a_l^\dagger | j_+ + j_- | a_m^\dagger \rangle \langle a_m^\dagger | j_+ + j_- | a_{l'}^\dagger \rangle \right. \\ &+ u_{m(l)} u_l(m) v_{l'(m)}^* v_{m(l')} \langle a_l^\dagger | j_+ + j_- | a_m^\dagger \rangle \langle a_m^\dagger | j_+ + j_- | a_{l'}^\dagger \rangle \\ &+ v_{m(l)}^* v_l(m) u_{l'(m)} u_{m(l')} \langle a_l^\dagger | j_+ + j_- | a_m^\dagger \rangle \langle a_m^\dagger | j_+ + j_- | a_{l'}^\dagger \rangle \\ &\left. + v_{m(l)}^* v_l(m) v_{l'(m)}^* v_{m(l')} \langle a_l^\dagger | j_+ + j_- | a_m^\dagger \rangle \langle a_m^\dagger | j_+ + j_- | a_{l'}^\dagger \rangle \right] \end{aligned} \quad (1.27)$$

$$\begin{aligned} &\sum_m \langle \varphi_l | j_+ + j_- | m \rangle \langle m | j_+ + j_- | \varphi_{l'} \rangle \\ &= \sum_m c_l^* c_{l'} \left(u_{m(l)} u_l(m) + v_{m(l)}^* v_l(m) \right) \left(u_{l'(m)} u_{m(l')} + v_{l'(m)}^* v_{m(l')} \right) \\ &\times \langle a_l^\dagger | j_+ + j_- | a_m^\dagger \rangle \langle a_m^\dagger | j_+ + j_- | a_{l'}^\dagger \rangle \\ &= \sum_m c_l^* c_{l'} \left(u_{m(l)} u_l(m) + v_{m(l)}^* v_l(m) \right) \left(u_{l'(m)} u_{m(l')} + v_{l'(m)}^* v_{m(l')} \right) \\ &\left[\langle a_l^\dagger | j_+ | a_m^\dagger \rangle \langle a_m^\dagger | j_+ | a_{l'}^\dagger \rangle + \langle a_l^\dagger | j_- | a_m^\dagger \rangle \langle a_m^\dagger | j_+ | a_{l'}^\dagger \rangle \right. \\ &\left. + \langle a_l^\dagger | j_+ | a_m^\dagger \rangle \langle a_m^\dagger | j_- | a_{l'}^\dagger \rangle + \langle a_l^\dagger | j_- | a_m^\dagger \rangle \langle a_m^\dagger | j_- | a_{l'}^\dagger \rangle \right] \end{aligned} \quad (1.28)$$

But,

$$\begin{aligned}
& \frac{1}{i^2} \sum_m \langle \varphi_l | j_+ - j_- | m \rangle \langle m | j_+ - j_- | \varphi_{l'} \rangle \\
&= - \sum_m c_l^* c_{l'} \left(u_{m(l)} u_{l(m)} + v_{m(l)}^* v_{l(m)} \right) \left(u_{l'(m)} u_{m(l')} + v_{l'(m)}^* v_{m(l')} \right) \\
&\times \langle a_l^+ | j_+ - j_- | a_m^+ \rangle \langle a_m^+ | j_+ - j_- | a_{l'}^+ \rangle \\
&= - \sum_m c_l^* c_{l'} \left(u_{m(l)} u_{l(m)} + v_{m(l)}^* v_{l(m)} \right) \left(u_{l'(m)} u_{m(l')} + v_{l'(m)}^* v_{m(l')} \right) \\
& \left[\langle a_l^+ | j_+ | a_m^+ \rangle \langle a_m^+ | j_+ | a_{l'}^+ \rangle - \langle a_l^+ | j_- | a_m^+ \rangle \langle a_m^+ | j_+ | a_{l'}^+ \rangle \right. \\
& \left. - \langle a_l^+ | j_+ | a_m^+ \rangle \langle a_m^+ | j_- | a_{l'}^+ \rangle + \langle a_l^+ | j_- | a_m^+ \rangle \langle a_m^+ | j_- | a_{l'}^+ \rangle \right]
\end{aligned}$$

If the two previous expressions are summed together, one finds

$$\begin{aligned}
& \sum_m \langle \varphi_l | j_+ + j_- | m \rangle \langle m | j_+ + j_- | \varphi_{l'} \rangle + \frac{1}{i^2} \sum_m \langle \varphi_l | j_+ - j_- | m \rangle \langle m | j_+ - j_- | \varphi_{l'} \rangle \\
&= 2 \sum_m c_l^* c_{l'} \left(u_{m(l)} u_{l(m)} + v_{m(l)}^* v_{l(m)} \right) \left(u_{l'(m)} u_{m(l')} + v_{l'(m)}^* v_{m(l')} \right) \\
& \left[\langle a_l^+ | j_- | a_m^+ \rangle \langle a_m^+ | j_+ | a_{l'}^+ \rangle + \langle a_l^+ | j_+ | a_m^+ \rangle \langle a_m^+ | j_- | a_{l'}^+ \rangle \right]
\end{aligned} \tag{1.29}$$

The completion relation is realized through the summation over the wave functions of all the intrinsic states a^+ , but is not directed by the wave functions b^+ which includes the rotational functions $\mathcal{D}_{M\Omega}^I(\omega)$. Finally, the relations read by indexing with the numbers Ω, m as

$$\begin{aligned}
& \sum_m \langle \varphi_l | j_+ + j_- | m \rangle \langle m | j_+ + j_- | \varphi_{l'} \rangle + \frac{1}{i^2} \sum_m \langle \varphi_l | j_+ - j_- | m \rangle \langle m | j_+ - j_- | \varphi_{l'} \rangle \\
&= 2 \sum_{\Omega} \sum_{m', m'', m} c_{\Omega, m''}^* c_{\Omega, m} \\
& \times \left(u_{\Omega-1, m'}(\Omega, m'') u_{\Omega, m''}(\Omega-1, m') + v_{\Omega-1, m'}^*(\Omega, m'') v_{\Omega, m''}(\Omega-1, m') \right) \\
& \times \left(u_{\Omega, m}(\Omega-1, m') u_{\Omega-1, m'}(\Omega, m) + v_{\Omega, m}^*(\Omega-1, m') v_{\Omega-1, m'}(\Omega, m) \right) \\
& \langle a_{\Omega, m''}^+ | j_+ | a_{\Omega-1, m'}^+ \rangle \langle a_{\Omega-1, m'}^+ | j_- | a_{\Omega, m}^+ \rangle \\
& + 2 \sum_{\Omega} \sum_{m', m'', m} c_{\Omega, m''}^* c_{\Omega, m} \\
& \times \left(u_{\Omega+1, m'}(\Omega, m'') u_{\Omega, m''}(\Omega+1, m') + v_{\Omega+1, m'}^*(\Omega, m'') v_{\Omega, m''}(\Omega+1, m') \right) \\
& \times \left(u_{\Omega, m}(\Omega+1, m') u_{\Omega+1, m'}(\Omega, m) + v_{\Omega, m}^*(\Omega+1, m') v_{\Omega+1, m'}(\Omega, m) \right) \\
& \langle a_{\Omega, m''}^+ | j_- | a_{\Omega+1, m'}^+ \rangle \langle a_{\Omega+1, m'}^+ | j_+ | a_{\Omega, m}^+ \rangle
\end{aligned} \tag{1.30}$$

The expected values of the energy functional is then:

$$\begin{aligned}
& \langle \varphi_{IM} | H + H_R - i\hbar \frac{\partial}{\partial t} + H' - \lambda N | \varphi_{IM} \rangle \\
&= \sum_{\Omega, m} |c_{\Omega, m}|^2 \left\{ 2 \sum_{(\Omega', m') \neq (\Omega, m)} |v_{\Omega', m'(\Omega, m)}|^2 (\epsilon_{\Omega', m'} - \lambda) + (\epsilon_{\Omega, m} - \lambda) \right. \\
&\quad - G \left| \sum_{(\Omega', m') \neq (\Omega, m)} u_{\Omega', m'(\Omega, m)} v_{\Omega', m'(\Omega, m)} \right|^2 - G \sum_{(\Omega', m') \neq (\Omega, m)} |v_{\Omega', m'(\Omega, m)}|^4 \left. \right\} \\
&+ \frac{\hbar^2}{2J} \sum_{\Omega, m} |c_{\Omega, m}|^2 [I(I+1) - \Omega^2] \\
&+ \frac{\hbar^2}{2J} \left\{ \frac{1}{2} \sum_{\Omega} \sum_{m', m'', m} c_{\Omega, m'}^* c_{\Omega, m} \right. \\
&\quad \times (u_{\Omega-1, m''(\Omega, m')} u_{\Omega, m'(\Omega-1, m'')} + v_{\Omega-1, m''(\Omega, m')}^* v_{\Omega, m'(\Omega-1, m'')}) \\
&\quad \times (u_{\Omega, m(\Omega-1, m'')} u_{\Omega-1, m''(\Omega, m)} + v_{\Omega, m(\Omega-1, m'')}^* v_{\Omega-1, m''(\Omega, m)}) \\
&\quad \times \langle a_{\Omega, m'}^+ | j_+ | a_{\Omega-1, m''}^+ \rangle \langle a_{\Omega-1, m''}^+ | j_- | a_{\Omega, m}^+ \rangle \\
&\quad + \frac{1}{2} \sum_{\Omega} \sum_{m', m'', m} c_{\Omega, m'}^* c_{\Omega, m} \\
&\quad \times (u_{\Omega+1, m''(\Omega, m')} u_{\Omega, m'(\Omega+1, m'')} + v_{\Omega+1, m''(\Omega, m')}^* v_{\Omega, m'(\Omega+1, m'')}) \\
&\quad \times (u_{\Omega, m(\Omega+1, m'')} u_{\Omega+1, m''(\Omega, m)} + v_{\Omega, m(\Omega+1, m'')}^* v_{\Omega+1, m''(\Omega, m)}) \\
&\quad \times \langle a_{\Omega, m'}^+ | j_- | a_{\Omega+1, m''}^+ \rangle \langle a_{\Omega+1, m''}^+ | j_+ | a_{\Omega, m}^+ \rangle \left. \right\} \\
&- \frac{\hbar^2}{2J} \left\{ \sum_{\Omega=-I, I} \sum_{m', m} c_{\Omega+1, m'}^* c_{\Omega, m} ((I-\Omega)(I+\Omega+1))^{1/2} \right. \\
&\quad \times \left[u_{\Omega, m(\Omega+1, m')} u_{\Omega+1, m'(\Omega, m)} + v_{\Omega, m(\Omega+1, m')}^* v_{\Omega+1, m'(\Omega, m)} \right] \\
&\quad \times \langle a_{\Omega+1, m'}^+ | j_+ | a_{\Omega, m}^+ \rangle \\
&\quad + \sum_{\Omega=-I, I} \sum_{m', m} c_{\Omega-1, m'}^* c_{\Omega, m} ((I+\Omega)(I-\Omega+1))^{1/2} \\
&\quad \times \left[u_{\Omega, m(\Omega-1, m')} u_{\Omega-1, m'(\Omega, m)} + v_{\Omega, m(\Omega-1, m')}^* v_{\Omega-1, m'(\Omega, m)} \right] \\
&\quad \times \langle a_{\Omega-1, m'}^+ | j_- | a_{\Omega, m}^+ \rangle \left. \right\} \\
&- i\hbar \sum_{\Omega, m} |c_{\Omega, m}|^2 \left[\sum_{(\Omega', m') \neq (\Omega, m)} \frac{1}{2} (v_{\Omega', m'(\Omega, m)}^* \dot{v}_{\Omega', m'(\Omega, m)} - \dot{v}_{\Omega', m'(\Omega, m)}^* v_{\Omega', m'(\Omega, m)}) \right] \\
&- i\hbar \sum_{\Omega, m} c_{\Omega, m}^* \dot{c}_{\Omega, m} + \sum_{\Omega, m, m'}^n h_{\Omega, m', m} c_{\Omega, m'}^* c_{\Omega, m}
\end{aligned} \tag{1.31}$$

In order to minimize the functional, the expression (1.31) is derived with respect to the independent variables $v_{l(m)}$ and $v_{l(m)}^*$ by taking into account the subsidiary condition $u_k^2 + v_k^2 = 1$. Two relations follows, one being

$$\begin{aligned}
& \sum_m^n |c_m|^2 \left\{ 2v_{l(m)}^* (\epsilon_l - \lambda_m) \right. \\
& - G \left[\sum_{k \neq m} \kappa_{k(m)} \left(-\frac{v_{l(m)}^* v_{l(m)}}{2u_{l(m)}} \right) + \left(u_{l(m)} - \frac{\rho_{l(m)}}{2u_{l(m)}} \right) \right. \\
& \quad \times \left. \left. \sum_{k \neq m} \kappa_{k(m)}^* + 2\rho_{l(m)} v_{l(m)}^* \right] + i\hbar \dot{v}_{l(m)}^* \right\} = 0,
\end{aligned} \tag{1.32}$$

and the other being its complex conjugate. This system can be solved by considering that the expression in the curly bracket is zero for each value of m . The time-dependent pairing equations associated to an unpaired nucleon in the state m emerge if no configuration mixings are allowed [146, 147]:

$$i\hbar \dot{\rho}_{l(m)} = \kappa_{l(m)} \Delta_m^* - \kappa_{l(m)}^* \Delta_m, \tag{1.33}$$

$$i\hbar\dot{\kappa}_{l(m)} = (2\rho_{l(m)} - 1) \Delta_m + 2\kappa_{l(m)} (\epsilon_l - \lambda_m) - 2G\rho_{l(m)}\kappa_{l(m)}. \quad (1.34)$$

Now, within the same expected value of the functional, it is possible to obtain the equations for the mixing of configurations. These equations are similar to the equations needed to obtain the probability that an unpaired nucleon is located on a state m . For this purpose, the expression (1.31) must be derived with respect c_m and c_m^* . Two equations follow, one being:

$$\begin{aligned} -i\hbar\dot{c}_{\Omega,m}^* &= c_{\Omega,m}^* \left\{ 2 \sum_{(\Omega',m') \neq (\Omega,m)} |v_{\Omega',m'}(\Omega,m)|^2 (\epsilon_{\Omega',m'} - \lambda) + (\epsilon_{\Omega,m} - \lambda) \right. \\ &- G \left| \sum_{(\Omega',m') \neq (\Omega,m)} u_{\Omega',m'}(\Omega,m) v_{\Omega',m'}(\Omega,m) \right|^2 - G \sum_{(\Omega',m') \neq (\Omega,m)} |v_{\Omega',m'}(\Omega,m)|^4 \left. \right\} \\ &+ \frac{\hbar^2}{2J} c_{\Omega,m}^* [I(I+1) - \Omega^2] \\ &+ \frac{\hbar^2}{2J} \left\{ \frac{1}{2} \sum_{m',m''} c_{\Omega,m'}^* (u_{\Omega-1,m''}(\Omega,m') u_{\Omega,m'}(\Omega-1,m'') + v_{\Omega-1,m''}^*(\Omega,m') v_{\Omega,m'}(\Omega-1,m'')) \right. \\ &\times (u_{\Omega,m}(\Omega-1,m'') u_{\Omega-1,m''}(\Omega,m) + v_{\Omega,m}^*(\Omega-1,m'') v_{\Omega-1,m''}(\Omega,m)) \\ &\times \langle a_{\Omega,m'}^+ | j+ | a_{\Omega-1,m''}^+ \rangle \langle a_{\Omega-1,m''}^+ | j- | a_{\Omega,m}^+ \rangle \\ &+ \frac{1}{2} \sum_{m',m''} c_{\Omega,m'}^* (u_{\Omega+1,m''}(\Omega,m') u_{\Omega,m'}(\Omega+1,m'') + v_{\Omega+1,m''}^*(\Omega,m') v_{\Omega,m'}(\Omega+1,m'')) \\ &\times (u_{\Omega,m}(\Omega+1,m'') u_{\Omega+1,m''}(\Omega,m) + v_{\Omega,m}^*(\Omega+1,m'') v_{\Omega+1,m''}(\Omega,m)) \\ &\times \langle a_{\Omega,m'}^+ | j- | a_{\Omega+1,m''}^+ \rangle \langle a_{\Omega+1,m''}^+ | j+ | a_{\Omega,m}^+ \rangle \left. \right\} \\ &- \frac{\hbar^2}{2J} \left\{ \sum_{m'} c_{\Omega+1,m'}^* ((I-\Omega)(I+\Omega+1))^{1/2} \right. \\ &\times \left[u_{\Omega,m}(\Omega+1,m') u_{\Omega+1,m'}(\Omega,m) + v_{\Omega,m}^*(\Omega+1,m') v_{\Omega+1,m'}(\Omega,m) \right] \langle a_{\Omega+1,m'}^+ | j+ | a_{\Omega,m}^+ \rangle \\ &+ \sum_{m'} c_{\Omega-1,m'}^* ((I+\Omega)(I-\Omega+1))^{1/2} \\ &\times \left[u_{\Omega,m}(\Omega-1,m') u_{\Omega-1,m'}(\Omega,m) + v_{\Omega,m}^*(\Omega-1,m') v_{\Omega-1,m'}(\Omega,m) \right] \langle a_{\Omega-1,m'}^+ | j- | a_{\Omega,m}^+ \rangle \left. \right\} \\ &- i\hbar c_{\Omega,m}^* \left[\sum_{(\Omega',m') \neq (\Omega,m)} \frac{1}{2} (v_{\Omega',m'}^*(\Omega,m) \dot{v}_{\Omega',m'}(\Omega,m) - \dot{v}_{\Omega',m'}^*(\Omega,m) v_{\Omega',m'}(\Omega,m)) \right] \\ &+ \sum_{\Omega,m'}^n \dot{h}_{\Omega,m' \neq m} c_{\Omega,m'}^* \end{aligned}$$

and the other being the complex conjugate. In the previous expression, the time derivative of $v_{\Omega',m'}(\Omega,m)$ intervenes. This derivative can be calculated by using the time-dependent pairing equations (1.32). The result is:

$$\begin{aligned} &\frac{i\hbar}{2} (v_{\Omega',m'}^*(\Omega,m) \dot{v}_{\Omega',m'}(\Omega,m) - \dot{v}_{\Omega',m'}^*(\Omega,m) v_{\Omega',m'}(\Omega,m)) \\ &= 2 |v_{\Omega',m'}(\Omega,m)|^2 (\epsilon_{\Omega',m'} - \lambda) - 2G |v_{\Omega',m'}(\Omega,m)|^4 \\ &+ \Re \left\{ \Delta_{\Omega,m}^* \left(\frac{|v_{\Omega',m'}(\Omega,m)|^4}{u_{\Omega',m'}(\Omega,m) v_{\Omega',m'}^*(\Omega,m)} - u_{\Omega',m'}(\Omega,m) v_{\Omega',m'}(\Omega,m) \right) \right\} \\ &= 2 |v_{\Omega',m'}(\Omega,m)|^2 (\epsilon_{\Omega',m'} - \lambda) - 2G |v_{\Omega',m'}(\Omega,m)|^4 \\ &+ \frac{u_{\Omega',m'}(\Omega,m) v_{\Omega',m'}(\Omega,m) \Delta_{\Omega,m}^* + u_{\Omega',m'}(\Omega,m) v_{\Omega',m'}^*(\Omega,m) \Delta_{\Omega,m}}{2} \left\{ \frac{|v_{\Omega',m'}(\Omega,m)|^4}{|u_{\Omega',m'}(\Omega,m) v_{\Omega',m'}(\Omega,m)|^2} - 1 \right\}, \end{aligned} \quad (1.35)$$

Therefore, the time-dependent equations for configuration mixing is obtained:

$$\begin{aligned}
-i\hbar\dot{c}_{\Omega,m}^* &= c_{\Omega,m}^* \left\{ (\epsilon_{\Omega,m} - \lambda) - \sum_{(\Omega',m') \neq (\Omega,m)} \right. \\
&\times \Re \left[\Delta_{\Omega,m}^* \left(\frac{|v_{\Omega',m'}(\Omega,m)|^4}{u_{\Omega',m'}(\Omega,m)v_{\Omega',m'}^*(\Omega,m)} - u_{\Omega',m'}(\Omega,m)v_{\Omega',m'}(\Omega,m) \right) \right] \\
&\left. - \frac{|\Delta_{\Omega,m}|^2}{G} + G \sum_{(\Omega',m') \neq (\Omega,m)} |v_{\Omega',m'}(\Omega,m)|^4 \right\} \\
&+ \frac{\hbar^2}{2J} c_{\Omega,m}^* [I(I+1) - \Omega^2] \\
&+ \frac{\hbar^2}{2J} \left\{ \frac{1}{2} \sum_{m',m''} c_{\Omega,m'}^* \left(u_{\Omega-1,m''}(\Omega,m') u_{\Omega,m'}(\Omega-1,m'') + v_{\Omega-1,m''}^*(\Omega,m') v_{\Omega,m'}(\Omega-1,m'') \right) \right. \\
&\times \left(u_{\Omega,m}(\Omega-1,m'') u_{\Omega-1,m''}(\Omega,m) + v_{\Omega,m}^*(\Omega-1,m'') v_{\Omega-1,m''}(\Omega,m) \right) \\
&\times \left\langle a_{\Omega,m'}^+ | j_+ | a_{\Omega-1,m''}^+ \right\rangle \left\langle a_{\Omega-1,m''}^+ | j_- | a_{\Omega,m}^+ \right\rangle \\
&+ \frac{1}{2} \sum_{m',m''} c_{\Omega,m'}^* \left(u_{\Omega+1,m''}(\Omega,m') u_{\Omega,m'}(\Omega+1,m'') + v_{\Omega+1,m''}^*(\Omega,m') v_{\Omega,m'}(\Omega+1,m'') \right) \\
&\times \left(u_{\Omega,m}(\Omega+1,m'') u_{\Omega+1,m''}(\Omega,m) + v_{\Omega,m}^*(\Omega+1,m'') v_{\Omega+1,m''}(\Omega,m) \right) \\
&\times \left\langle a_{\Omega,m'}^+ | j_- | a_{\Omega+1,m''}^+ \right\rangle \left\langle a_{\Omega+1,m''}^+ | j_+ | a_{\Omega,m}^+ \right\rangle \left. \right\} \\
&- \frac{\hbar^2}{2J} \left\{ \sum_{m'} c_{\Omega+1,m'}^* ((I - \Omega)(I + \Omega + 1))^{1/2} \right. \\
&\times \left[u_{\Omega,m}(\Omega+1,m') u_{\Omega+1,m'}(\Omega,m) + v_{\Omega,m}^*(\Omega+1,m') v_{\Omega+1,m'}(\Omega,m) \right] \times \left\langle a_{\Omega+1,m'}^+ | j_+ | a_{\Omega,m}^+ \right\rangle \\
&+ \sum_{m'} c_{\Omega-1,m'}^* ((I + \Omega)(I - \Omega + 1))^{1/2} \\
&\times \left[u_{\Omega,m}(\Omega-1,m') u_{\Omega-1,m'}(\Omega,m) + v_{\Omega,m}^*(\Omega-1,m') v_{\Omega-1,m'}(\Omega,m) \right] \left\langle a_{\Omega-1,m'}^+ | j_- | a_{\Omega,m}^+ \right\rangle \left. \right\} \\
&+ \sum_{\Omega,m'}^n h_{\Omega,m' \neq m} c_{\Omega,m'}^*
\end{aligned}$$

If the amplitude of a seniority-1 configuration is known, and the nuclear system evolves in time, the previous equations give us the amplitudes of all other seniority-1 configurations that are populated during the evolution of the system. All these seniority-1 configurations are connected by “gates” opened by the Landau-Zener and the Coriolis interactions. Of course, another system of equations is available for the complex conjugates of the amplitudes..

In general, in nuclear physics it is usual to speak about probabilities instead of amplitudes. The equations can be recasted to gives the probabilities instead of the amplitudes. Multiplying the Eq. (1.36) with c_m , its complex conjugates with c_m^* , and subtracting, the next relation follows.

$$\begin{aligned}
& i\hbar[\dot{c}_{\Omega,m}c_{\Omega,m}^* + \dot{c}_{\Omega,m}^*c_{\Omega,m}] \\
&= \frac{\hbar^2}{2J} \left\{ \frac{1}{2} \sum_{m',m''} [c_{\Omega,m'}c_{\Omega,m}^* - c_{\Omega,m'}^*c_{\Omega,m}] (u_{\Omega-1,m''(\Omega,m')} u_{\Omega,m'(\Omega-1,m'')} \right. \\
&\times v_{\Omega-1,m''(\Omega,m')}^* v_{\Omega,m'(\Omega-1,m'')}) \\
&\times (u_{\Omega,m(\Omega-1,m'')} u_{\Omega-1,m''(\Omega,m)} + v_{\Omega,m(\Omega-1,m'')}^* v_{\Omega-1,m''(\Omega,m)}) \\
&\times \langle a_{\Omega,m'}^+ | j_+ | a_{\Omega-1,m''}^+ \rangle \langle a_{\Omega-1,m''}^+ | j_- | a_{\Omega,m}^+ \rangle \\
&+ \frac{1}{2} \sum_{m',m''} [c_{\Omega,m'}c_{\Omega,m}^* - c_{\Omega,m'}^*c_{\Omega,m}] \\
&\times (u_{\Omega+1,m''(\Omega,m')} u_{\Omega,m'(\Omega+1,m'')} + v_{\Omega+1,m''(\Omega,m')}^* v_{\Omega,m'(\Omega+1,m'')}) \\
&\times (u_{\Omega,m(\Omega+1,m'')} u_{\Omega+1,m''(\Omega,m)} + v_{\Omega,m(\Omega+1,m'')}^* v_{\Omega+1,m''(\Omega,m)}) \\
&\times \langle a_{\Omega,m'}^+ | j_- | a_{\Omega+1,m''}^+ \rangle \langle a_{\Omega+1,m''}^+ | j_+ | a_{\Omega,m}^+ \rangle \left. \right\} \tag{1.36} \\
&- \frac{\hbar^2}{2J} \left\{ \sum_{m'} [c_{\Omega+1,m'}c_{\Omega,m}^* - c_{\Omega+1,m'}^*c_{\Omega,m}] ((I - \Omega)(I + \Omega + 1))^{1/2} \right. \\
&\times \left[u_{\Omega,m(\Omega+1,m')} u_{\Omega+1,m'(\Omega,m)} + v_{\Omega,m(\Omega+1,m')}^* v_{\Omega+1,m'(\Omega,m)} \right] \\
&\times \left\langle a_{\Omega+1,m'}^+ | j_+ | a_{\Omega,m}^+ \right\rangle \\
&+ \sum_{m'} [c_{\Omega-1,m'}c_{\Omega,m}^* - c_{\Omega-1,m'}^*c_{\Omega,m}] ((I + \Omega)(I - \Omega + 1))^{1/2} \\
&\times \left[u_{\Omega,m(\Omega-1,m')} u_{\Omega-1,m'(\Omega,m)} + v_{\Omega,m(\Omega-1,m')}^* v_{\Omega-1,m'(\Omega,m)} \right] \\
&\times \left\langle a_{\Omega-1,m'}^+ | j_- | a_{\Omega,m}^+ \right\rangle \left. \right\} \\
&+ \sum_{\Omega,m'}^n h_{\Omega,m' \neq m} [c_{\Omega,m'}c_{\Omega,m}^* - c_{\Omega,m'}^*c_{\Omega,m}]
\end{aligned}$$

From relations (1.36) and its complex conjugate, another relation can be deduced

$$\begin{aligned}
& i\hbar(\dot{c}_j^*c_m + \dot{c}_m c_j^*) \\
&= c_m c_j^* \left[-\frac{1}{G} (|\Delta_m|^2 - |\Delta_j|^2) + (\epsilon_m - \epsilon_j - \lambda_m + \lambda_j) \right. \\
&+ 2 \sum_{k \neq m} \rho_{k(m)} (\epsilon_k - \lambda_m) - 2 \sum_{k \neq j} \rho_{k(j)} (\epsilon_k - \lambda_j) \\
&\left. - G \left(\sum_{k \neq m} \rho_{k(m)}^2 - \sum_{k \neq j} \rho_{k(j)}^2 \right) \right] \tag{1.37} \\
&- \frac{i\hbar}{2} c_m \dot{c}_j^* \left[\sum_{k \neq m} (v_{k(m)}^* \dot{v}_{k(m)} - \dot{v}_{k(m)}^* v_{k(m)}) \right. \\
&- \sum_{k \neq j} (v_{k(j)}^* \dot{v}_{k(j)} - \dot{v}_{k(j)}^* v_{k(j)}) \left. \right] \\
&+ \sum_{l \neq m}^n h_{lm} c_l c_j^* - \sum_{l \neq j}^n h_{lj} c_l^* c_m.
\end{aligned}$$

The derivatives \dot{v} and \dot{v}^* are still kept in the previous expression to make the equations simpler. The Rel. (1.35) which is deduced from the time dependent pairing should be also recasted in terms of probabilities. The transformed relation follows:

$$\begin{aligned}
& \frac{i\hbar}{2} (v_{\Omega',m'}^* \dot{v}_{\Omega',m'} - \dot{v}_{\Omega',m'}^* v_{\Omega',m'}) \\
&= 2\rho_{\Omega',m'}(\Omega,m) (\epsilon_{\Omega',m'} - \lambda_{\Omega,m}) - 2G\rho_{\Omega',m'}^2(\Omega,m) \\
&+ \frac{\Delta_{\Omega,m}^*}{2} \left(\frac{\rho_{\Omega',m'}^2(\Omega,m)}{\kappa_{\Omega',m'}^*(\Omega,m)} - \kappa_{\Omega',m'}(\Omega,m) \right) + \frac{\Delta_{\Omega,m}}{2} \left(\frac{\rho_{\Omega',m'}^2(\Omega,m)}{\kappa_{\Omega',m'}(\Omega,m)} - \kappa_{\Omega',m'}^*(\Omega,m) \right) \quad (1.38) \\
&= 2\rho_{\Omega',m'}(\Omega,m) (\epsilon_{\Omega',m'} - \lambda_{\Omega,m}) - 2G\rho_{\Omega',m'}^2(\Omega,m) \\
&+ \Re \left\{ \Delta_{\Omega,m}^* \left(\frac{\rho_{\Omega',m'}^2(\Omega,m)}{\kappa_{\Omega',m'}^*(\Omega,m)} - \kappa_{\Omega',m'}(\Omega,m) \right) \right\}.
\end{aligned}$$

This last relation reveals the fact that the equations for configuration mixing depends not only on the interactions in the avoided crossing region and on the Coriolis coupling, but also on the dynamical occupation probabilities that are obtained for the same collective velocity. It is interesting to note that the expressions inferring the time derivatives of the BCS occupation amplitudes in Eq. (1.38) have energy dimensions.

The Rel (1.37) gives us the probabilities to find a seniority-1 configuration at a given deformation, for a given collective velocity. The second equation that can be deduced represent a moment component between different seniority-1 configurations:

$$\begin{aligned}
i\hbar[\dot{c}_{\Omega_1, m_1} c_{\Omega, m}^* + \dot{c}_{\Omega, m}^* c_{\Omega_1, m_1}] &= c_{\Omega_1, m_1} c_{\Omega, m}^* \left[\frac{\hbar^2}{2J} (\Omega^2 - \Omega_1^2) \right] \\
&- c_{\Omega_1, m_1} \frac{\hbar^2}{2J} \left\{ \frac{1}{2} \sum_{m', m''} c_{\Omega, m'}^* (u_{\Omega-1, m''}(\Omega, m') u_{\Omega, m'}(\Omega-1, m'') + v_{\Omega-1, m''}^*(\Omega, m') v_{\Omega, m'}(\Omega-1, m'')) \right. \\
&\times (u_{\Omega, m}(\Omega-1, m'') u_{\Omega-1, m''}(\Omega, m) + v_{\Omega, m}^*(\Omega-1, m'') v_{\Omega-1, m''}(\Omega, m)) \\
&\times \langle a_{\Omega, m'}^+ | j_+ | a_{\Omega-1, m''}^+ \rangle \langle a_{\Omega-1, m''}^+ | j_- | a_{\Omega, m}^+ \rangle \\
&+ \frac{1}{2} \sum_{m', m''} c_{\Omega, m'}^* (u_{\Omega+1, m''}(\Omega, m') u_{\Omega, m'}(\Omega+1, m'') + v_{\Omega+1, m''}^*(\Omega, m') v_{\Omega, m'}(\Omega+1, m'')) \\
&\times (u_{\Omega, m}(\Omega+1, m'') u_{\Omega+1, m''}(\Omega, m) + v_{\Omega, m}^*(\Omega+1, m'') v_{\Omega+1, m''}(\Omega, m)) \\
&\times \langle a_{\Omega, m'}^+ | j_- | a_{\Omega+1, m''}^+ \rangle \langle a_{\Omega+1, m''}^+ | j_+ | a_{\Omega, m}^+ \rangle \left. \right\} \\
&+ c_{\Omega, m}^* \frac{\hbar^2}{2J} \left\{ \frac{1}{2} \sum_{m', m''} c_{\Omega_1, m'} (u_{\Omega_1-1, m''}(\Omega_1, m') u_{\Omega_1, m'}(\Omega_1-1, m'') + v_{\Omega_1-1, m''}^*(\Omega_1, m') v_{\Omega_1, m'}(\Omega_1-1, m'')) \right. \\
&\times (u_{\Omega_1, m_1}(\Omega_1-1, m'') u_{\Omega_1-1, m''}(\Omega_1, m_1) + v_{\Omega_1, m_1}^*(\Omega_1-1, m'') v_{\Omega_1-1, m''}(\Omega_1, m_1)) \\
&\times \langle a_{\Omega_1, m'}^+ | j_+ | a_{\Omega_1-1, m''}^+ \rangle \langle a_{\Omega_1-1, m''}^+ | j_- | a_{\Omega_1, m_1}^+ \rangle \\
&+ \frac{1}{2} \sum_{m', m''} c_{\Omega_1, m'} (u_{\Omega_1+1, m''}(\Omega_1, m') u_{\Omega_1, m'}(\Omega_1+1, m'') + v_{\Omega_1+1, m''}^*(\Omega_1, m') v_{\Omega_1, m'}(\Omega_1+1, m'')) \\
&\times (u_{\Omega_1, m_1}(\Omega_1+1, m'') u_{\Omega_1+1, m''}(\Omega_1, m_1) + v_{\Omega_1, m_1}^*(\Omega_1+1, m'') v_{\Omega_1+1, m''}(\Omega_1, m_1)) \\
&\times \langle a_{\Omega_1, m'}^+ | j_- | a_{\Omega_1+1, m''}^+ \rangle \langle a_{\Omega_1+1, m''}^+ | j_+ | a_{\Omega_1, m_1}^+ \rangle \left. \right\} \\
&+ \frac{\hbar^2}{2J} c_{\Omega_1, m_1} \left\{ \sum_{m'} c_{\Omega+1, m'}^* ((I - \Omega)(I + \Omega + 1))^{1/2} \left[u_{\Omega, m}(\Omega+1, m') u_{\Omega+1, m'}(\Omega, m) + v_{\Omega, m}^*(\Omega+1, m') v_{\Omega+1, m'}(\Omega, m) \right] \right. \\
&\times \langle a_{\Omega+1, m'}^+ | j_+ | a_{\Omega, m}^+ \rangle \\
&+ \sum_{m'} c_{\Omega-1, m'}^* ((I + \Omega)(I - \Omega + 1))^{1/2} \left[u_{\Omega, m}(\Omega-1, m') u_{\Omega-1, m'}(\Omega, m) + v_{\Omega, m}^*(\Omega-1, m') v_{\Omega-1, m'}(\Omega, m) \right] \\
&\times \langle a_{\Omega-1, m'}^+ | j_- | a_{\Omega, m}^+ \rangle \left. \right\} \\
&- \frac{\hbar^2}{2J} c_{\Omega, m}^* \left\{ \sum_{m'} c_{\Omega_1+1, m'} ((I - \Omega_1)(I + \Omega_1 + 1))^{1/2} \left[u_{\Omega_1, m_1}(\Omega_1+1, m') u_{\Omega_1+1, m'}(\Omega_1, m_1) + v_{\Omega_1, m_1}^*(\Omega_1+1, m') v_{\Omega_1+1, m'}(\Omega_1, m_1) \right] \right. \\
&\times \langle a_{\Omega_1+1, m'}^+ | j_+ | a_{\Omega_1, m_1}^+ \rangle \\
&+ \sum_{m'} c_{\Omega_1-1, m'} ((I + \Omega_1)(I - \Omega_1 + 1))^{1/2} \left[u_{\Omega_1, m_1}(\Omega_1-1, m') u_{\Omega_1-1, m'}(\Omega_1, m_1) + v_{\Omega_1, m_1}^*(\Omega_1-1, m') v_{\Omega_1-1, m'}(\Omega_1, m_1) \right] \\
&\times \langle a_{\Omega_1-1, m'}^+ | j_- | a_{\Omega_1, m_1}^+ \rangle \left. \right\} \\
&+ c_{\Omega_1, m_1} c_{\Omega, m}^* \left\{ -\frac{1}{G} (|\Delta_{\Omega_1, m_1}|^2 - |\Delta_{\Omega, m}|^2) \right. \\
&+ (\epsilon_{\Omega_1, m_1} - \epsilon_{\Omega, m} - 2\lambda) \\
&+ G \left(\sum_{(\Omega', m') \neq (\Omega_1, m_1)} \rho_{\Omega', m'}^2(\Omega_1, m_1) - \sum_{(\Omega', m') \neq (\Omega, m)} \rho_{\Omega', m'}^2(\Omega, m) \right) \\
&- \sum_{(\Omega', m') \neq (\Omega_1, m_1)} \Re \left[\Delta_{\Omega_1, m_1}^* \left(\frac{\rho_{\Omega', m'}^2(\Omega_1, m_1)}{\kappa_{\Omega', m'}^*(\Omega_1, m_1)} - \kappa_{\Omega', m'}(\Omega_1, m_1) \right) \right] \\
&+ \sum_{(\Omega', m') \neq (\Omega, m)} \Re \left[\Delta_{\Omega, m}^* \left(\frac{\rho_{\Omega', m'}^2(\Omega, m)}{\kappa_{\Omega', m'}^*(\Omega, m)} - \kappa_{\Omega', m'}(\Omega, m) \right) \right] \left. \right\} \\
&+ \sum_{(\Omega', m') \neq (\Omega, m), (\Omega_1, m_1)}^n h_{(\Omega_1, m_1)}(\Omega', m') c_{\Omega', m'}^* c_{\Omega, m}^* - \sum_{(\Omega', m') \neq (\Omega, m), (\Omega_1, m_1)}^n h_{(\Omega', m')}(\Omega, m) c_{\Omega', m'}^* c_{\Omega_1, m_1} \\
&+ h_{(\Omega_1, m_1)}(\Omega, m) c_{\Omega, m} c_{\Omega, m}^* - h_{(\Omega, m)}(\Omega_1, m_1) c_{\Omega_1, m_1}^* c_{\Omega_1, m_1}.
\end{aligned} \tag{1.39}$$

After some rearrangements of terms, and defining the moment components of the probabilities $S_{(\Omega, m)(\Omega_1, m_1)} = c_{\Omega, m}^* c_{\Omega_1, m_1}$ and transforming the Rels. (1.37) and (1.39), the Eqs. (1.40) and (1.41) are eventually obtained. These equations de-

pend on the single particle densities and the pairing moment components. So we obtain the dependence in time of the seniority-1 probabilities and of their mixing components. The equations follows:

$$\begin{aligned}
i\hbar\dot{P}_{\Omega,m} = & \frac{\hbar^2}{2J} \left\{ \frac{1}{2} \sum_{m',m''} \left[S_{(\Omega,m)(\Omega,m')} - S_{(\Omega,m')(\Omega,m)} \right] \right. \\
& \times \left(u_{\Omega-1,m''(\Omega,m')} u_{\Omega,m'(\Omega-1,m'')} + v_{\Omega-1,m''(\Omega,m')}^* v_{\Omega,m'(\Omega-1,m'')} \right) \\
& \times \left(u_{\Omega,m(\Omega-1,m'')} u_{\Omega-1,m''(\Omega,m)} + v_{\Omega,m(\Omega-1,m'')}^* v_{\Omega-1,m''(\Omega,m)} \right) \\
& \times \left\langle a_{\Omega,m'}^+ | j_+ | a_{\Omega-1,m''}^+ \right\rangle \left\langle a_{\Omega-1,m''}^+ | j_- | a_{\Omega,m}^+ \right\rangle \\
& + \frac{1}{2} \sum_{m',m''} \left[S_{(\Omega,m)(\Omega,m')} - S_{(\Omega,m')(\Omega,m)} \right] \\
& \times \left(u_{\Omega+1,m''(\Omega,m')} u_{\Omega,m'(\Omega+1,m'')} + v_{\Omega+1,m''(\Omega,m')}^* v_{\Omega,m'(\Omega+1,m'')} \right) \\
& \times \left(u_{\Omega,m(\Omega+1,m'')} u_{\Omega+1,m''(\Omega,m)} + v_{\Omega,m(\Omega+1,m'')}^* v_{\Omega+1,m''(\Omega,m)} \right) \\
& \times \left\langle a_{\Omega,m'}^+ | j_- | a_{\Omega+1,m''}^+ \right\rangle \left\langle a_{\Omega+1,m''}^+ | j_+ | a_{\Omega,m}^+ \right\rangle \left. \right\} \\
& - \frac{\hbar^2}{2J} \left\{ \sum_{m'} \left[S_{(\Omega,m)(\Omega+1,m')} - S_{(\Omega+1,m')(\Omega,m)} \right] ((I-\Omega)(I+\Omega+1))^{1/2} \right. \\
& \times \left[u_{\Omega,m(\Omega+1,m')} u_{\Omega+1,m'(\Omega,m)} + v_{\Omega,m(\Omega+1,m')}^* v_{\Omega+1,m'(\Omega,m)} \right] \times \left\langle a_{\Omega+1,m'}^+ | j_+ | a_{\Omega,m}^+ \right\rangle \\
& + \sum_{m'} \left[S_{(\Omega,m)(\Omega-1,m')} - S_{(\Omega-1,m')(\Omega,m)} \right] ((I+\Omega)(I-\Omega+1))^{1/2} \\
& \times \left[u_{\Omega,m(\Omega-1,m')} u_{\Omega-1,m'(\Omega,m)} + v_{\Omega,m(\Omega-1,m')}^* v_{\Omega-1,m'(\Omega,m)} \right] \left\langle a_{\Omega-1,m'}^+ | j_- | a_{\Omega,m}^+ \right\rangle \left. \right\} \\
& + \sum_{\Omega,m'}^n h_{\Omega,m' \neq m} \left[S_{(\Omega,m)(\Omega,m')} - S_{(\Omega,m')(\Omega,m)} \right], \tag{1.40}
\end{aligned}$$

and

$$\begin{aligned}
i\hbar\dot{S}_{(\Omega,m)(\Omega_1,m_1)} &= S_{(\Omega,m)(\Omega_1,m_1)} \left[\frac{\hbar^2}{2J}(\Omega^2 - \Omega_1^2) \right] - \frac{\hbar^2}{2J} \times \left\{ \frac{1}{2} \sum_{m',m''} S_{(\Omega,m')(\Omega_1,m_1)} \right. \\
&\times \left(u_{\Omega-1,m''}(\Omega,m') u_{\Omega,m'(\Omega-1,m'')} + v_{\Omega-1,m''}^*(\Omega,m') v_{\Omega,m'(\Omega-1,m'')} \right) \\
&\times \left(u_{\Omega,m(\Omega-1,m'')} u_{\Omega-1,m''}(\Omega,m) + v_{\Omega,m(\Omega-1,m'')}^* v_{\Omega-1,m''}(\Omega,m) \right) \\
&\times \left\langle a_{\Omega,m'}^+ | j_+ | a_{\Omega-1,m''}^+ \right\rangle \left\langle a_{\Omega-1,m''}^+ | j_- | a_{\Omega,m}^+ \right\rangle \\
&+ \frac{1}{2} \sum_{m',m''} S_{(\Omega,m')(\Omega_1,m_1)} \left(u_{\Omega+1,m''}(\Omega,m') u_{\Omega,m'(\Omega+1,m'')} + v_{\Omega+1,m''}^*(\Omega,m') v_{\Omega,m'(\Omega+1,m'')} \right) \\
&\times \left(u_{\Omega,m(\Omega+1,m'')} u_{\Omega+1,m''}(\Omega,m) + v_{\Omega,m(\Omega+1,m'')}^* v_{\Omega+1,m''}(\Omega,m) \right) \\
&\times \left\langle a_{\Omega,m'}^+ | j_- | a_{\Omega+1,m''}^+ \right\rangle \left\langle a_{\Omega+1,m''}^+ | j_+ | a_{\Omega,m}^+ \right\rangle \left. \right\} + \frac{\hbar^2}{2J} \left\{ \frac{1}{2} \sum_{m',m''} S_{(\Omega,m)(\Omega_1,m')} \right. \\
&\times \left(u_{\Omega_1-1,m''}(\Omega_1,m') u_{\Omega_1,m'(\Omega_1-1,m'')} + v_{\Omega_1-1,m''}^*(\Omega_1,m') v_{\Omega_1,m'(\Omega_1-1,m'')} \right) \\
&\times \left(u_{\Omega_1,m_1(\Omega_1-1,m'')} u_{\Omega_1-1,m''}(\Omega_1,m_1) + v_{\Omega_1,m_1(\Omega_1-1,m'')}^* v_{\Omega_1-1,m''}(\Omega_1,m_1) \right) \\
&\times \left\langle a_{\Omega_1,m'}^+ | j_+ | a_{\Omega_1-1,m''}^+ \right\rangle \left\langle a_{\Omega_1-1,m''}^+ | j_- | a_{\Omega_1,m_1}^+ \right\rangle + \frac{1}{2} \sum_{m',m''} S_{(\Omega,m)(\Omega_1,m')} \\
&\left(u_{\Omega_1+1,m''}(\Omega_1,m') u_{\Omega_1,m'(\Omega_1+1,m'')} + v_{\Omega_1+1,m''}^*(\Omega_1,m') v_{\Omega_1,m'(\Omega_1+1,m'')} \right) \\
&\times \left(u_{\Omega_1,m_1(\Omega_1+1,m'')} u_{\Omega_1+1,m''}(\Omega_1,m_1) + v_{\Omega_1,m_1(\Omega_1+1,m'')}^* v_{\Omega_1+1,m''}(\Omega_1,m_1) \right) \\
&\times \left. \left\langle a_{\Omega_1,m'}^+ | j_- | a_{\Omega_1+1,m''}^+ \right\rangle \left\langle a_{\Omega_1+1,m''}^+ | j_+ | a_{\Omega_1,m_1}^+ \right\rangle \right\} \\
&+ \frac{\hbar^2}{2J} \left\{ \sum_{m'} S_{(\Omega+1,m')(\Omega_1,m_1)} ((I - \Omega)(I + \Omega + 1))^{1/2} \right. \\
&\times \left[u_{\Omega,m(\Omega+1,m')} u_{\Omega+1,m'}(\Omega,m) + v_{\Omega,m(\Omega+1,m')}^* v_{\Omega+1,m'}(\Omega,m) \right] \left\langle a_{\Omega+1,m'}^+ | j_+ | a_{\Omega,m}^+ \right\rangle \\
&+ \sum_{m'} S_{(\Omega-1,m')(\Omega_1,m_1)} ((I + \Omega)(I - \Omega + 1))^{1/2} \\
&\times \left[u_{\Omega,m(\Omega-1,m')} u_{\Omega-1,m'}(\Omega,m) + v_{\Omega,m(\Omega-1,m')}^* v_{\Omega-1,m'}(\Omega,m) \right] \left\langle a_{\Omega-1,m'}^+ | j_- | a_{\Omega,m}^+ \right\rangle \left. \right\} \\
&- \frac{\hbar^2}{2J} \left\{ \sum_{m'} S_{(\Omega,m)(\Omega_1+1,m')} ((I - \Omega_1)(I + \Omega_1 + 1))^{1/2} \right. \\
&\times \left[u_{\Omega_1,m_1(\Omega_1+1,m')} u_{\Omega_1+1,m'}(\Omega_1,m_1) + v_{\Omega_1,m_1(\Omega_1+1,m')}^* v_{\Omega_1+1,m'}(\Omega_1,m_1) \right] \\
&\times \left\langle a_{\Omega_1+1,m'}^+ | j_+ | a_{\Omega_1,m_1}^+ \right\rangle + \sum_{m'} S_{(\Omega,m)(\Omega_1-1,m')} ((I + \Omega_1)(I - \Omega_1 + 1))^{1/2} \\
&\times \left[u_{\Omega_1,m_1(\Omega_1-1,m')} u_{\Omega_1-1,m'}(\Omega_1,m_1) + v_{\Omega_1,m_1(\Omega_1-1,m')}^* v_{\Omega_1-1,m'}(\Omega_1,m_1) \right] \\
&\times \left. \left\langle a_{\Omega_1-1,m'}^+ | j_- | a_{\Omega_1,m_1}^+ \right\rangle \right\} + S_{(\Omega,m)(\Omega_1,m_1)} \left\{ -\frac{1}{G} \left(|\Delta_{\Omega_1,m_1}|^2 - |\Delta_{\Omega,m}|^2 \right) \right. \\
&+ (\epsilon_{\Omega_1,m_1} - \epsilon_{\Omega,m} - 2\lambda) \\
&+ G \left(\sum_{(\Omega',m') \neq (\Omega_1,m_1)} \rho_{\Omega',m'}^2(\Omega_1,m_1) - \sum_{(\Omega',m') \neq (\Omega,m)} \rho_{\Omega',m'}^2(\Omega,m) \right) \\
&- \sum_{(\Omega',m') \neq (\Omega_1,m_1)} \Re \left[\Delta_{\Omega_1,m_1}^* \left(\frac{\rho_{\Omega',m'}^2(\Omega_1,m_1)}{\kappa_{\Omega',m'}^*(\Omega_1,m_1)} - \kappa_{\Omega',m'}(\Omega_1,m_1) \right) \right] \\
&+ \sum_{(\Omega',m') \neq (\Omega,m)} \Re \left[\Delta_{\Omega,m}^* \left(\frac{\rho_{\Omega',m'}^2(\Omega,m)}{\kappa_{\Omega',m'}^*(\Omega,m)} - \kappa_{\Omega',m'}(\Omega,m) \right) \right] \left. \right\} \\
&+ \sum_{(\Omega',m') \neq (\Omega,m), (\Omega_1,m_1)}^n h_{(\Omega_1,m_1)(\Omega',m')} S_{(\Omega,m)(\Omega',m')} \\
&- \sum_{(\Omega',m') \neq (\Omega,m), (\Omega_1,m_1)}^n h_{(\Omega',m')(\Omega,m)} S_{(\Omega',m')(\Omega_1,m_1)} \\
&+ h_{(\Omega_1,m_1)(\Omega,m)} P_{\Omega,m} - h_{(\Omega,m)(\Omega_1,m_1)} P_{\Omega_1,m_1}.
\end{aligned} \tag{1.41}$$

These equations should be solved numerically by knowing the single particle states, the Landau-Zener and the Coriolis couplings. Simple examples with solutions of these generalized time dependent pairing equations are given in the following section.

4 Results

This section addresses several examples concerning the applications of the previous relations in fission dynamics. The first example concerns the fission of ^{232}Th as investigated in Ref. [159]. By using the time-dependent pairing equations given by Eqs. (1.33) and (1.34), it is possible to determine the fission times. This system of coupled equations are able to infer the excitation energy at scission as function of the internuclear velocity between the two nascent fragments. By comparing the theoretical values of the dissipated energies and the experimental ones, the best value of the internuclear velocity is obtained. By knowing the collective velocity and the shape of the barrier, the determination of the fission time is determined in an obvious way.

But, in order to solve the system of the equations of motion, the single particle levels diagrams are required for the protons and neutrons configurations. That is, a disintegration path, the single particle diagrams, and some models to calculate the inertia, are required. First of all we need to know how the single particle levels are rearranged during fission, how they react to the change of the mean field. Usually, it is considered that the nuclear mean field is managed by some generalized coordinates, which correspond to the most important degrees of freedom of the system. The generalized coordinates vary in time leading to the scission. So, a nuclear shape parametrization is the main ingredient needed in our calculations. In the examples given in this work, the nuclear shape parametrization is axial symmetric, being a combination of two ellipsoids of different semi-axis smoothly joined by an intermediate surface given by the rotation of an arc of circle around the axis of symmetry. This nuclear shape parametrization depends on five degrees of freedom: the elongation, the mass-asymmetry, the necking, the deformations of both fragments. The elongation is denoted R , being the distance between the centers of the spheroids. The mass asymmetry is denoted a_1/a_2 , that is the ratio of the major semi axis of the two nascent fragments. The necking is represented by C_3 , the curvature of the arc of circle that defines the intermediate surface. The deformations of the fragments are b_1/a_1 and b_2/a_2 , that is the ratio between the semi-axis of the fragments 1 and 2, respectively. The essential problem is to find a trajectory in the configuration space spanned by our five independent generalized coordinates that starts from the ground state and arrives at the scission, where the two complementary fragments are formed. For this purpose, one determines numerically a path in the configuration space within the algorithm proposed in Ref. [149], in which the dependencies of the parameters a_1/a_2 , C_3 , b_1/a_1 and b_2/a_2 are obtained as function of R . This path

should minimize the penetrability given by the WKB formula

$$P = \exp \left\{ \frac{2}{\hbar} \int \sqrt{[V(R) - E_0]B(R)} dr \right\} \quad (1.42)$$

where $V(R)$ is the deformation energy, $B(R)$ is the inertia and E_0 is the zero point kinetic energy. The macroscopic-microscopic model [150, 151] is used to calculate the deformation energy. In this model, a combination between a liquid drop energy and shell effect offers a good estimation of the total energy of the nucleus as function of the deformation parameters. To calculate the liquid drop part, several contributions are taken into account: the Coulomb energy, the surface term which is given by the Yukawa-plus-exponential interaction [152], the Coulomb diffuseness correction contribution, the volume term, and the Wigner one. The formulas for these contributions entering in the calculation of the liquid drop energy are presented in Ref. [153]. At scission, the model is generalized for binary systems with different charge densities [154]. The shell and pairing effects constituting the microscopic corrections are calculated by using the Strutinsky procedure [155]. By using this method, the rapid fluctuating effects due to the intrinsic structure can be inferred in the total energy of the nuclear system. The fissioning nuclear system acquires a potential that has a double humped shape. The intermediate well is responsible for the resonances that appear in the structure of the fission cross section, as displayed in Fig. 1 and explained in the text. The inertia along the least action trajectory is

$$B(R) = \sum_{q_1} \sum_{q_2} B_{q_1 q_2} \frac{\partial q_1}{\partial R} \frac{\partial q_2}{\partial R} \quad (1.43)$$

where q_1 and q_2 are two generalized coordinates, and $B_{q_1 q_2}$ is the element of the mass tensor versus q_1 and q_2 . This symmetric tensor describes the reaction of the nuclear system towards the external forces which modify the generalized coordinates q_i . The tensor of inertia can be obtained from the variational principle as given in Refs. [84, 135, 140]. In Ref. [140], the behavior of the inertia for the nucleus investigated in this example is described. The main generalized coordinate in our model is the elongation (or the internuclear distance) R defined as the distance between the centers of the two nascent fragments.

Once the fission path is obtained in the configuration space it is possible to calculate the single particle diagrams required to solve the equations of motion given by Eqs. (1.33) and (1.34). The single particle levels were calculated within the Woods-Saxon two center shell model [141]. This model is able to describe the passage from one nucleus into two separated bodies in a very accurate way, being useful to characterize scission configurations [156, 157, 158]. Even more, this precision also holds true for very large mass-asymmetries, as obtained in the case of alpha or cluster decay [160, 161, 162, 163]. In our model, the ground state of ^{224}Th is deformed, the fundamental elongation being $R \approx 4$ fm. The scission point of the Th

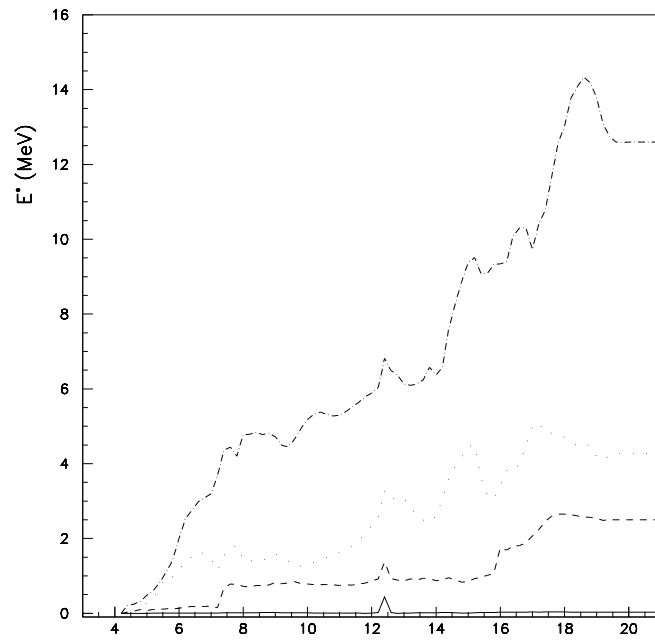


Figure 3: Dissipated energy as function of the internuclear distance R for four tunneling velocities. Full line $dR/dt = 1 \times 10^4$ fm/fs, dashed line $dR/dt = 1 \times 10^5$ fm/fs, dot-dashed line $dR/dt = 1 \times 10^6$ fm/fs, and dotted line $dR/dt = 1 \times 10^7$ fm/fs. Figure adapted from reference [159]

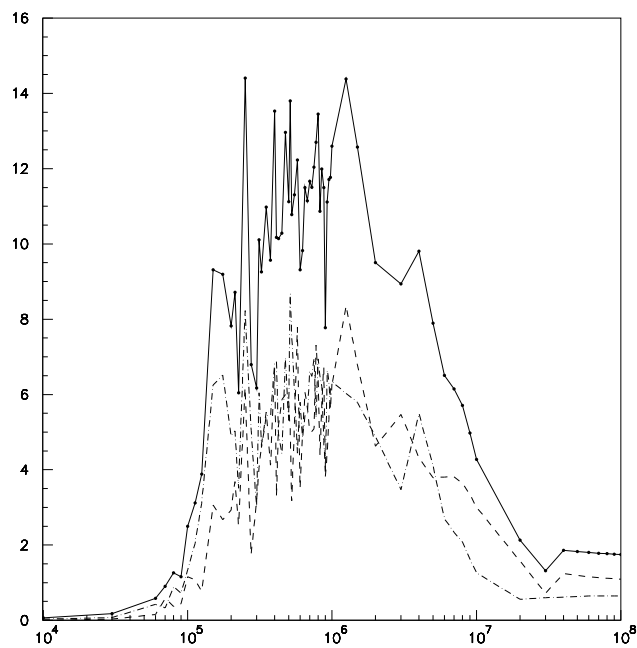


Figure 4: Dissipated energy at scission as function of the tunneling velocity $v = dR/dt$. Dot-dashed line neutron dissipated energy, dashed line proton dissipated energy and full line total dissipated energy. Figure adapted from reference [159]

nucleus is located somewhere at $R \approx 19$ fm. Details about these calculations can be found in Ref. [149].

The time-dependent pairing equation were solved beginning from the ground state up to the scission configuration spanning an interval of tunneling velocities $v = dR/dt$ comprised between 1×10^4 and 1×10^8 fm/fs. The initial values of the single particle densities and of the pairing moment components are taken as the BCS amplitudes for the stationary state. The variation of the dissipated energies are plotted in Figs. 3 and 4 for a pairing model with a constant strength G . First of all, it can be noticed that the dissipated energy increases especially in the region of the outer fission barrier, between $R=14$ and $R=18$ fm. This increase of the dissipated energy in the region of the second barrier is more pronounced in the case of state dependent pairing, as it can be seen in Ref. [159], but the behavior is similar to the case presented in this work. As expected, in both formalism the dissipated energy remains unchanged after the scission point. After scission the rearrangement of the single particle levels ceases, and the time dependent pairing equations become stationary. Therefore, the dissipated energy remains constant. Because, many values of the dissipated energy are tested, it is now possible to select the collective velocity that pertain to the dissipated energy which infers the experimental data. The dissipated energy for the 1×10^4 fm/fs tunneling velocity is negligible. That is, for a very slow deformation of the nuclear system, the nuclear fission process behaves adiabatically. A such value of the dissipated energy corresponds to cold fission processes, in which the excitation energy at scission is so small that no neutron are emitted. very large. That is, the nuclear systems proceeds through adiabatic states. For nuclear velocities that amount to the order of 1×10^6 fm/fs, the dissipated energy is very large. That is, the nuclear systems proceeds through diabatic states. The dissipated energy amounts to 14 MeV, this values being sufficient to emit at least two neutrons from the evaporation from the fission fragments. For tunneling velocities larger than 1×10^7 fm/fs, the final dissipated energy decreases and arrives on a plateau. This happens because we reached the limit of validity of our model. For these large velocities, the passage from the ground state to the scission point is too rapid, the occupation probabilities cannot be modified and the system arrives at scission with occupation probabilities close to the initial ones. Statistically, the Fermi energy of the a nuclear system is roughly about 40 MeV. Accordingly, an average nucleon velocity of 8×10^7 fm/fs can be associated to the Fermi energy of the nucleons. To allow a rearrangement of the nuclear states, the internuclear velocity should be much smaller than the velocity of the nucleons inside the nucleus. Otherwise the nucleons have not the possibility to accommodate with the variations of the mean field.

In Ref. [149] it is shown that for the two pairing mechanisms investigated, the dissipated energy have a maximal value around a velocity of 1×10^6 fm/fs. The striking difference between the two models is the fact that the dissipated energy amounts up to 70 MeV in the case of the state-dependent pairing mechanism.

As mentioned above, the cold fission is a process in which the dissipated energy is so low that no neutrons can be emitted. So, a dissipated energy of 6 MeV, approaching the binding energy of the neutron, can be considered as an upper value which characterizes the cold fission processes. From the Fig. 4 where the dependence of the dissipated energy at scission is displayed versus the collective velocity, the corresponding velocities for an excitation energy of 6 MeV can be inferred as 1.3×10^5 fm/fs. It should be noted that it was remarked in Ref. [149] that the tunneling velocity is much lower for the state dependent pairing. In fission, the intrinsic excitation energies at scission are measured from the number of evaporated neutrons from the fission fragments, and it is considered to be around 10 MeV for most of the parent nuclei [164]. In this work it is considered that in thermal fission the mean dissipation amounts about 12 MeV. For this reasonable value of the dissipated energy, one deduced that the corresponding velocities range in a small interval $[4 \times 10^6 - 1.5 \times 10^6]$ fm/fs for a constant pairing strength. A smallest value was also estimated of about 1.2×10^6 fm/fs for a state dependent pairing interactions. From the behavior of the deformation energy versus the elongation, a shift of the elongation of about 3 fm between the top of the external barrier and the scission point was considered. Once this distance available, it is possible to evaluate the time for the descent of the barrier. This time has the following values. In order to obtain 6 MeV dissipated energy at scission, it is $T = 2 \times 10^{-20}$ s, while in order to have 12 MeV at scission, it is about 2×10^{-21} s.

We concluded that the tunneling times that can be obtained from calculations for the fission processes are strongly model dependent. A realistic pairing interaction produce a fission time considerably longer than a constant pairing interaction. The fission process could very fast or very slow in superfluid systems to reproduce the same value of an observable, depending on the behavior of the pairing interaction.

Another example concerning the influence of the dynamics of fission is related to the pair breaking mechanism. The system of differential equations (1.40) and (1.41) can be modified by taking into account a pair breaking mechanism, as done in Ref. [157]. In general it is accredited that in cold fission, the distributions of the masses of the fission fragments are even-even, due to the the pairing mechanism influence [165, 166]. Accordingly, at very low excitation energies, the fragments would be fully paired. Very low excitation energies of the fragments are translated in high kinetic energies that approach the Q -value of the reaction. A pioneering experiment, obtained after improving the experimental procedure, contradicted this commonly accepted behavior. In the data of Ref. [167] a first step was achieved: no strong even-odd effect was evidenced in the thermal neutron induced fission for high values of the total kinetic energy. Surprisingly, even and odd partitions were observed experimentally close to their respective Q values for four systems investigated: $^{233,235}\text{U}(n_{th},f)$, $^{239}\text{Pu}(n_{th},f)$ and $^{252}\text{Cf}(sf)$. An even more strange behavior was observed in Refs, [168, 169, 170]. The experimental data exhibited higher odd-odd fission yields at excitation energies smaller than 4-6 MeV than even-even ones.

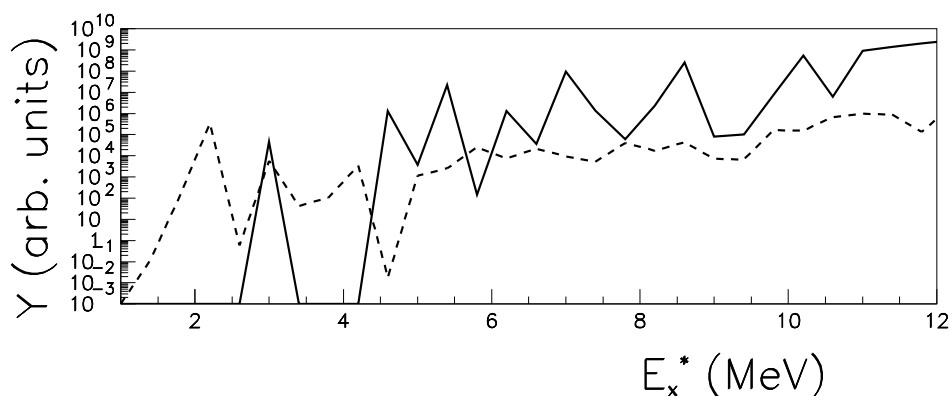


Figure 5: The dependence of the even-even fission yield as function of the dissipated energy is plotted with a full line. The dependence of the odd-odd fission yield as function of the dissipated energy is plotted with a broken line. Figure adapted from reference [157]

That lead us to consider the importance of the Landau-Zener effect in the cold-fission fragmentation, as mentioned in Ref. [157]. In this case, as a result of the interaction in an avoided levels crossing region it is possible to break a pair by using dynamical considerations. However, without introducing the dynamics, the odd-even structure in fission is explained usually within statistical arguments, as for example in Refs. [171, 172, 173]. It is also possible to take into account some arguments linked the odd-even structure and to the excitation energy during the fission process [175, 176, 177, 178].

The fission yields as function of the total excitation energy for the fragmentation $^{90}\text{Kr} + ^{144}\text{Ba}$ (even-even), $^{90}\text{Rb} + ^{144}\text{Cs}$ (odd-odd) is investigated theoretically by solving the time dependent pairing equations, generalized by including the Landau-Zener effect and the Coriolis coupling. For this reaction, experimental data are available for the reaction $^{233}\text{U}(n_{th},f)$ [168], allowing us to test the model.

When the odd-odd partition are treated, the barrier must be larger by adding the value of the excitation energy of the unpaired nucleons. That leads to a decrease of the fission penetrability. Wheeler introduced this specialization energy in Ref. [179]. The fission path was obtained in the framework of the least action principle, obtaining the most probable fragmentation. By calculating the single particle levels diagrams, the ingredients required to solve the equations of motion are obtained. A pairing active level space of 58 levels around the Fermi energy was selected. The avoided crossing levels regions were identified. After that, one selected 32 seniority two configurations for protons and 31 configurations for neutrons that are coupled to the seniority zero configuration through avoided levels crossings regions. Several values of the internuclear velocity $v = \dot{R}$ are tested in order to solve the

generalized time dependent pairing equations: 5×10^2 , 8×10^2 , 10^3 , 3×10^3 , 10^4 , 3×10^4 , 10^5 , 3×10^5 , 10^6 , and 3×10^6 fm/fs. The ground state configurations of the stationary values of the BCS amplitudes were taken as initial conditions to solve the equations of motion. The probability to retrieve the system in the ground state in a seniority-0 configuration was taken as $P_0=1$. A typical behavior for all the seniority-2 configurations was remarked. The general rule exhibits a proportionality between the dissipated energy at scission and the collective velocity.

The final probabilities of realization of all seniority configurations for neutrons and protons as function of the internuclear velocities are displayed were obtained after solving the equations of motion. The results evidence a curious behavior: the probability of realization of the adiabatic seniority-0 states are close to zero for small velocities, exactly in the energy region in which the dissipation is smaller. From these theoretical results it is possible to understand the main features concerning the relation between the final excitation energy and the probability of realization of a given channel. If the probability of realization of a seniority-0 configuration, that, for the even-even partition is very small at low excitation energies, implicitly the probabilities of realization of odd-odd partitions or seniority-2 configurations is much larger. The final results are plotted in Fig. 5 by folding on small interval of the excitation energy the probabilities of the odd-odd configurations. So, a strange experimental result was obtained: at low excitation energy the odd-odd yields surpass the even-even ones. The even-even yields become larger for excitation energies larger than 3-4 MeV. This strange experimental result was explained from dynamics.

Through a dynamical analysis and solving the microscopic equations of motion for a fissioning even-even system it is found that the probability to obtain an odd-odd partition overcomes the probability of an even-even one at excitation energies smaller than 4 MeV, for the same division in mass numbers. The theoretical results are in accordance with the experimental behavior of the odd-even distributions at high kinetic energies. It is the first time that this behavior was explained within a quantum-mechanical approach.

5 Instead of conclusion

Today, an increased interest is focused in developing new cycles for nuclear power plants which is determined especially by social needs linked to security. It is crucial to ensure the safety of nuclear power plants and to handle with responsibility the nuclear wastes. As mentioned before, the nuclear fission is still unsatisfactory understood. A better knowledge of the fission mechanism should be realized in order to reduce the risks of the nuclear power plants and to design the new generations. One solution is to improve our knowledge on the Th fission. Although thorium itself cannot support a nuclear chain reaction, by bombarding thorium to a flux of neutrons inside a nuclear reactor, converts this element to uranium 233, which can support

fission. For this reasons, the design of nuclear plants have long time considered the possibility of a fuel given by a combination of thorium with a fissionable isotope, which would initiate the reaction. For this purpose, a better modeling and experimental determination of cross-section evaluations were needed in the actinide and sub-actinide region. As mentioned, actual evaluations are mainly phenomenological, the heights of the double fission barrier being determined empirically in accordance with a given parameterization of the nuclear level density. This procedure does not include the resonance due to the beta vibrational and rotational coupling adequately. Also, fission of actinides as well as sub-actinides is not yet understood sufficiently for increasing energies above a few MeV. Some efforts must be also involved in a better experimental determination of nuclear data by improving the experimental concepts and configurations. Fundamental research in the field of nuclear physics is necessary to improve our knowledge. The final goal is to obtain values of the neutron-induced cross sections within an accuracy of several percents while actually the error bars are of almost 30%. So, any theoretical project in fission dynamics is according to such efforts. In principle, apart a developments of the theoretical models, the nuclear research is also focused towards a better determination of nuclear properties of nuclei by understanding better the nuclear fission mechanism in order to provide more reliable data. The economic importance for fission can be evidenced briefly in the following. The production of nuclear energy requires a combustible able to furnish energy through fission. Between the nuclei constituting the combustible we must distinguish among two main types: the fissile nuclei able to fission after a thermal neutron capture and the fertile nuclei that lead to a fissile nucleus after the capture of a neutron followed by several beta disintegration. The main fissile nuclei are ^{233}U , ^{235}U , ^{239}Pu and ^{241}Pu . The main fertile nuclei are ^{232}Th and ^{238}U . The last ones are abundant in the nature and the extraction is not very difficult. Among the fissile nuclei, only ^{235}U can be found in nature. Actually, the U-cycle is imposed as the most important way to produce nuclear energy due to historical consideration (the first nuclear reactor constructed under the guidance of Enrico Fermi in 1942) and due to the development of nuclear weapons. The combustible is obtained by mixing two isotopes of uranium (235 and 238). Some drawbacks are raised by the U-cycle. The first one is linked to the criticality of the actual reactors. The consequences of the Tchernobyl accident were proved disastrous. Secondly, the administration of the nuclear wastes is another important problem. Thirdly, the resources are limited, the abundance of ^{235}U is only 0.72% of the natural uranium Improved reactor types are needed because uranium resources are available only for 30 y with the actual utilization [180]. In such conditions, another cycle based on a mixing of ^{233}U and ^{232}Th becomes recently very promising for the nuclear energy production, namely the Th-cycle. Unfortunately, this cycle has also some drawbacks. A lot of investment and fundamental researches must be realized in the field. The project of such hybrid reactor is launched at European and International levels. As mentioned in the Ref. [181] a complex European project started to propose a technological route

to reduce the risks associated to nuclear waste, route based on transmutation in ADS. it is necessary to determine accurately the fission and capture cross sections for ^{233}Pa , ^{230}Th , ^{232}Th and the trans-uranium elements. These cross sections must be known at least within an accuracy of 15%. Actually, the evaluations obtained for these nuclei give a precision smaller than 30%. In the case of ^{232}Th the cross section accuracy is required to be about of 2 % and in the case of ^{233}U a value of 1% is necessary. This last isotope supplies the main exothermic reaction of the cycle. More over, the actinide data are scarce and often discrepant, especially for ^{232}Th and ^{233}U and must be supplemented by further experimental studies. Due to the lack of knowledge in the field, most countries abandoned this Th scheme decades ago, but increasing concerns about the diversion of plutonium from spent nuclear fuel to the construction of nuclear weapons has prompted reexamination. IAEA has maintained an interest in the thorium fuel cycle that offers the previous advantages. Momentary, the following fission cross sections must be improved: $^{232-234}\text{U}$, $^{230-234}\text{Pa}$ and $^{230-233}\text{Th}$. The most important requirements can be classified as follows: determination of the basic cross-sections, evaluation of available experimental data to compute cross-sections and improvements of actual models. The largest activities in Europe concerning these goals are coordinated within the n_TOF project and cover experimental measurements and cross-sections and model evaluations. The activities plan to improve the understanding of the mechanism of fission in order to improve the cross section evaluations.

References

- [1] O. Hahn and F. Strassmann, *Naturewiss* **27**, 11 (1939)
- [2] L. Meitner and O. R. Frisch, *Nature* **143**, 239 (1939)
- [3] N. Bohr and J. A. Wheeler, *Phys. Rev.* **56**, 426 (1939)
- [4] D. L. Hill and J. A. Wheeler, *Phys. Rev.* **89**, 1102 (1953)
- [5] S. G. Nilsson, *Mat. Fys. Medd. Dan. Vid. Selsk* **29**, 1 (1955).
- [6] J. Maruhn and W. Greiner, *Z. Phys.* **251**, 431 (1972)
- [7] R. D. Woods and D. S. Saxon, *Phys. Rev.* **95**, 577 (1954)
- [8] E. Rost, *Phys. Lett. B* **26**, 184 (1968)
- [9] B. N. Schunck and L. M. Robledo, *Rep. Prog. Phys.* **79**, 116301 (2016)
- [10] A. M. Lane and R. G. Thomas *Rev. Mod. Phys.* **30**, 257 (1958)
- [11] R. G. Moore *Rev. Mod. Phys.* **32**, 101 (1960)

- [12] H. Feshbach, C. E. Porter, and V. F. Weisskopf, *Phys. Rev.* **96**, 448 (1954)
- [13] G. N. Flerov, A. A. Pleve, S. M. Polikanov, S. P. Tretyakova, N. Martalogu, D. Poenaru, M. Sezon, I. Vilcov, and N. Vilcov, *Nucl. Phys. A* **97**, 444 (1967)
- [14] G. N. Flerov, A. A. Pleve, S. M. Polikanov, S. P. Tretyakova, I. Boca, M. Sezon, I. Vilcov, and N. Vilcov, *Nucl. Phys. A* **102**, 443 (1967)
- [15] D. Paya, J. Blons, H. Derrien, A. Michaudon, and P. Ribon, *J. Phys. (Paris)* **29**, 159 (1968)
- [16] E. Migneco and J. P. Theobald, *Nucl. Phys. A* **112**, 603 (1968)
- [17] M. Holmberg, L. G. Stromberg, and L. Wallin, *Nucl. Phys. A* **127**, 149 (1969)
- [18] V. M. Strutinsky, *Nucl. Phys. A* **122**, 1 (1968)
- [19] M. Brack, J. Damgaard, A. S. Jensen, H. C. Pauli, V. M. Strutinsky, and C. Y. Wong, *Rev. Mod. Phys.* **44**, 320 (1972)
- [20] H. C. Pauli, *Phys. Rep.* **7**, 35 (1973)
- [21] I. Grant, *Rep. Prog. Phys.* **39**, 955 (1976)
- [22] J. R. Nix, *Ann. Rev. Nucl. Sci.* **22**, 65 (1972)
- [23] The Plutonium Project, *Rev. Mod. Phys.* **18**, 513 (1946)
- [24] L. E. Glendenin, E. P. Steinberg, M. G. Inghram, and D. C. Hess, *Phys. Rev.* **84**, 860 (1951)
- [25] V. V. Pashkevich, *Nuclear Physics A* **169**, 275 (1971)
- [26] A. C. Wahl, *At. Data Nucl. Data Tabl.* **39**, 1 (1988)
- [27] B. D. Wilkins, E. P. Steinberg, and R. R. Chasman, *Phys. Rev. C* **14**, 1832 (1976)
- [28] U. Brosa, H.-H. Knitter, T.-S. Fan, J.-M. Hu, and S.-L. Bao, *Phys. Rev. C* **59**, 767 (1999)
- [29] P. Armbruster, *Rep. Prog. Phys.* **62**, 465 (1999)
- [30] H.-G. Clerc, W. Lang, M. Mutterer, C. Schmitt, J. P. Theobald, U. Quade, K. Rudolph, P. Armbruster, F. Gonnenwein, H. Schrader, and D. Engelhardt, *Nucl. Phys. A* **452**, 277 (1986)
- [31] F. Gonnenwein and B. Borsig, *Nucl. Phys. A* **530**, 27 (1991)
- [32] P. Fong, *Phys. Rev. C* **13**, 1259 (1976)

- [33] R. W. Hasse, Nucl. Phys. A **128**, 609 (1969)
- [34] J. Maruhn and W. Greiner, Phys. Rev. Lett. **32**, 548 (1974)
- [35] J. Randrup and P. Moller, Phys. Rev. Lett. **106**, 132503 (2011)
- [36] A. J. Sierk, Phys. Rev. C **96**, 034603 (2017)
- [37] J. Terrell, Phys. Rev. **113**, 527 (1959)
- [38] J. Terrel, Phys. Rev. **127**, 880 (1962)
- [39] V. F. Apalin, Y. N. Gritsyuk, I. E. Kutinov, V. I. Lebedev, and L.A. Mikaelian, Nuc. Phys. **71**, 553 (1965)
- [40] S. L. Whestone, Phys. Rev. **114** 581 (1959)
- [41] R. Vandenbosch, Nuc. Phys. **46**, 129 (1963)
- [42] J. C. D. Milton and J. S. Fraser, Phys. Rev. Lett. **7**, 67 (1961)
- [43] M. Mirea, Phys. Rev. C **83**, 054608 (2011)
- [44] R. Capote, Y.-J. Chen, F.-J. Hamsch, N. V. Kornilov, J. P. Lestone, O. Litaize, B. Morillon, D. Neudecker, S. Oberstedt, T. Ohsawa, N. Otuka, V. G. Pronyaev, A. Saxena, O. Serot, O. A. Shcherbakov, N.-C. Shu, D. Smith, P. Talou, A. Trkov, A. C. Tudora, R. Vogt, and A. S. Vorobyev, Nucl. Data. Sheets **131**, 1 (2016)
- [45] D. G. Madland and J. R. Nix, Nucl. Sci. Eng. **81**, 213 (1982)
- [46] A. Tudora and F.-J. Hamsch, Eur. Phys. J. A **53**, 159 (2017)
- [47] A. J. Sierk, Phys. Rev. C **33**, 2039 (1986)
- [48] A. Bohr, *On the theory of nuclear fission* (Proceedings of the International Conference on the Peaceful of the Atomic Energy, 8-20 August 1955, vol. 2, Geneva, Switzerland, p. 155, United Nation, New York, 1956)
- [49] S. Bjornholm and V. M. Strutinsky, Nucl. Phys. A **136**, 1 (1969)
- [50] I. Halpern and V. M. Strutinsky, *Angular distributions in particle induced fission at medium energies* (Proceedings of Second United Nations International Conference on the Peaceful Uses of Atomic Energy, 1-13 September 1958, vol. 15, Geneva, Switzerland, p. 408, United Nation, Geneva, 1958)
- [51] J. J. Griffin, Phys. Rev. **116**, 107 (1959)
- [52] K. Mazurek, P. N. Nadtochny, E. G. Ryabov, and G. D. Adeev, Eur. Phys. J. A **53**, 79 (2017)

- [53] R. Vandenbosch, *Phys. Rev. C* **7**, 2092 (1973)
- [54] F.A. Ivanyuk, C. Ishizuka, M.D. Usang, and S. Chiba, *Phys. Rev. C* **97** 054331 (2018)
- [55] U. Mosel and H.W. Schmitt, *Phys. Rev. C* **4**, 2185 (1971)
- [56] R. Chaudhry, R. Vandenbosch, and J. R. Huizenga, *Phys. Rev.* **126**, 220 (1962)
- [57] J. J. Griffin, *Phys. Rev.* **132**, 2204 (1963)
- [58] I. Ahmad and W. R. Phillips, *Rep. Prog. Phys.* **58**, 1415 (1995)
- [59] J. B. Wilhelmy, E. Cheifetz, R. C. Jared, S. G. Thompson, H. R. Bowman, and J. O. Rasmussen, *Phys. Rev. C* **5**, 20141 (1972)
- [60] A. V. Karpov, R. M. Hiryanov, A. V. Sagdeev, and G. D. Adeev, *J. Phys. G* **34**, 255 (2007)
- [61] H. J. Specht *Rev. Mod. Phys.* **46**, 773 (1974)
- [62] S. M. Polikanov, *Sov. Phys. Usp.* **15**, 486 (1973)
- [63] G. F. Auchampaugh and L. W. Weston, *Phys. Rev. C* **12**, 1850 (1975)
- [64] M. S. Moore, J. D. Moses, G. A. Keyworth, J. W. T. Dabbs, and N. W. Hill, *Phys. Rev. C* **18**, 1328 (1978)
- [65] W. J. Swiatecki, *Phys. Rev.* **101**, 97 (1956)
- [66] A. Sandulescu and W. Greiner, *Rep. Prog. Phys.* **55**, 1423 (1992)
- [67] A. N. Andreyev, J. Elseviers, M. Huyse, P. Van Duppen, S. Antalic, A. Barzakh, N. Bree, T. E. Cocolios, V. F. Comas, J. Diriken, D. Fedorov, V. Fedosseev, S. Franchoo, J. A. Heredia, O. Ivanov, U. Koster, B. A. Marsh, K. Nishio, R. D. Page, N. Patronis, M. Seliverstov, I. Thsekhanovich, J. Van den Bergh, P. Van DeWalle, M. Venhart, S. Vermote, M. Veselsky, C. Wagemans, T. Ichikawa, A. Iwamoto, P. Moller, and A. J. Sierk, *Phys. Rev. Lett.* **105**, 252502 (2010)
- [68] P. Moller, J. Randrup, and A. J. Sierk, *Phys. Rev. Lett.* **82**, 024306 (2012)
- [69] A. N. Andreyev, K. Nishio, and K.-H. Schmidt, *Rep. Prog. Phys.* **81**, 016301 (2018)
- [70] E. K. Hulet, J. F. Wild, R. J. Dougan, R. W. Lougheed, J. H. Landrum, A. D. Dougan, M. Schadel, R. L. Hahn, P. A. Baisden, C. M. Henderson, R. J. Dupzyk, K. Summerer, and G. R. Bethume, *Phys. Rev. Lett.* **56**, 313 (1986)

- [71] W. Schwab, H.-G. Clerc, J. P. Mutterer, J. P. Theobald, and H. Faust, Nucl. Phys. A **577**, 674 (1994)
- [72] F.-J. Hambsch, H. H. Knitter, and C. Budtz-Jorgensen, Nucl. Phys. A **574**, 209 (1993)
- [73] M. Mirea, Phys. Lett. B **680**, 316 (2009)
- [74] G. F. Bertsch, W. Loveland, W. Nazarewicz, and P. Talou, J. Phys. G **42**, 077001 (2015)
- [75] J. D. Cramer and J. R. Nix, Phys. Rev. C **2**, 1048 (1970)
- [76] A. R. Junghans, M. de Jong, H.-G. Clerc, A. V. Ignatyuk, G. A. Kudyaev, and K.-H. Schmidt, Nucl. Phys. A **629**, 635 (1998)
- [77] C. E. Porter and R. G. Thomas, Phys. Rev. **104**, 483 (1956)
- [78] D. C. Hoffman and M. R. Lane, Radiochim. Acta **70/71**, 135 (1995)
- [79] J. Blons, C. Mazur, D. Paya, M. Ribrag, and H. Weigmann, Phys. Rev. Lett. **19**, 1282 (1978)
- [80] J. Blons, Nucl. Phys. A **502**, 121c (1989)
- [81] P. Moller, Nucl. Phys. A **192**, 529 (1972)
- [82] M. Mirea, L. Tassan-Got, C. Stephan, C. O. Bacri, and R. C. Bobulescu, Europhys. Lett. **73**, 705 (2006)
- [83] H. Hofmann, Phys. Lett. B **42**, 177 (1972)
- [84] M. Mirea, J. Phys. G **43**, 105103 (2016)
- [85] L. Wilets, Phys. Rev. **116**, 372 (1959)
- [86] A. S. Jensen and J. Damgaard, Nucl. Phys. A **203**, 578 (1973)
- [87] P. Talou, T. Kawano, M. P. Chadwick, D. Neudecker, and M. E. Rising, J. Phys. G **42**, 034025 (2015)
- [88] S. Bjornholm and J. E. Lynn, Rev. Mod. Phys. **52**, 725 (1980)
- [89] A. J. Koning and D. Rochman, Nucl. Data Sheets **113**, 2012 (2012)
- [90] R. Capote, M. Herman, P. Oblozinsky, P. G. Young, S. Goriely, T. Belgya, A. V. Ignatyuk, A. J. Konong, S. Hilaire, V. A. Plujko, M. Avrigeanu, O. Bersillon, M. B. Chadwick, T. Fukahori, Z. Ge, Y. Han, S. Kailas, J. Kopecky, V. M. Maslov, G. Reffo, M. Sin, E. S. Soukhovitskii, and P. Talou, Nucl. Data Sheets **110**, 3107 2009

- [91] N. Colonna, A. Tsinganis, R. Vlastou, N. Patronis, M. Diakaki, S. Amaducci, M. Barbagallo, S. Bennett, E. Berthoumieux, M. Bacak, G. Cosentino, S. Cristallo, P. Finocchiaro, J. Heyse, D. Lewis, A. Manna, C. Massimi, E. Mendoza, M. Mirea, A. Moens, R. Nolte, E. Pirovano, M. Sabate-Gilarte, G. Sibbens, A.G. Smith, N. Sosnin, A. Stamatopoulos, D. Tarrío, L. Tassan-Got, D. Vanleeuw, A. Ventura, D. Vescovi, T. Wright, and P. Zugec, *Eur. Phys. J. A* **56**, 48 (2020)
- [92] E. Bauge, G. Belier, J. Cartier, A. Chatillon, J. M. Daugas, J. P. Delaroche, P. Dossantos-Uzarralde, H. Duarte, N. Dubray, M. Ducauze-Philippe, L. Gaudefroy, G. Gosselin, T. Granier, S. Hilaire, P. C. Huu-Tai, J. M. Laborie, B. Laurent, X. Ledoux, C. Le Luel, V. Meot, P. Morel, B. Morillon, O. Roig, P. Romain, J. Taieb, C. Varignon, N. Authier, P. Casoli, and B. Richard, *Eur. Phys. J. A* **48**, 113 (2012)
- [93] K. H. Schmidt and B. Jurado, *Eur. Phys. J. A* **51**, 176 (2015)
- [94] K. H. Schmidt, B. Jurado, C. Amouroux, and C. Schmitt, *Nucl. Data Sheets* **131**, 107 (2016)
- [95] W. D. Myers and W. J. Swiatecki, *Nucl. Phys. A* **601**, 141 (1996)
- [96] B. Jurado and K.-H. Schmidt, *J. Phys. G* **42**, 055101 (2015)
- [97] H. J. Krappe and K. Pomorski, *Lecture Note in Physics* **838**, 1 (2012)
- [98] K.-H. Schmidt and B. Jurado, *Prog. Rep. Phys.* **81**, 106301 (2018)
- [99] P. A. Seeger and W. H. Howard, *Phys. Lett. B* **57**, 7 (1975)
- [100] P. Moller and J. Nix, *At. Data. Nucl. Data Tabl.* **39**, 213 (1988)
- [101] P. Moller, A. J. Sierk, and A. Iwamoto, *Phys. Rev. Lett.* **92**, 072501 (2004)
- [102] M. Mirea and L. Tassan-Got, *Cent. Eur. J. Phys.* **9**, 116 (2011)
- [103] A. Dobrowolski, K. Pomorski, and J. Bartel, *Phys. Rev. C* **75**, 024613 (2017)
- [104] J. R. Nix, *Annu. Rev. Nucl. Sci.* **22**, 65 (1972)
- [105] M. Bolsterli, E. O. Fiset, J. R. Nix, and J. L. Norton, *Phys. Rev. C* **5**, 1050 (1972)
- [106] P. Quentin and H. Flocard, *Ann. Rev. Nucl. Sci.* **28**, 523 (1978)
- [107] J. W. Negele and D. Vautherin, *Phys. Rev. C* **5**, 1472 (1972)
- [108] J. W. Negele, *Rev. Mod. Phys.* **54**, 913 (1982)
- [109] M. Bender, P. H. Heene, and P. G. Reinhard, *Rev. Mod. Phys.* **75**, 121 (2003)

- [110] T. Niksic, D. Vretenar, and P. Ring, *Prog. Part. Nucl. Phys.* **66**, 519 (2011)
- [111] B.-N. Lu, E.-G. Zhao, and S.-G. Zhou, *Phys. Rev. C* **85**, 011301(R) (2012)
- [112] A. Bulgac, P. Magierski, K. J. Roche, and I. Sfetcu, *Phys. Rev. Lett.* **116**, 122504 (2016)
- [113] R. R. Chasman, *Phys. Rev. C* **14**, 1935 (1976)
- [114] J. Dobaczewski, W. Nazarewicz, T. R. Werner, J. F. Berger, C. R. Chinn, and J. Decharge, *Phys. Rev. C* **53**, 2809 (1996)
- [115] M. Bender, K. Rutz, P.-G. Reinhard, and J. A. Maruhn, *Eur. Phys. J. A* **8**, 59 (2000)
- [116] M. Mirea and A. Sandulescu, *Rom. Rep. Phys.* **70**, 201 (2017)
- [117] J. F. Berger, M. Girod, and D. Gogny, *Nucl. Phys. A* **502**, 85c (1989)
- [118] M. Bender, K. Rutz, P.-G. Reinhard, and J. A. Maruhn, *Eur. Phys. J. A* **7**, 467 (2000)
- [119] S. Goriely, M. Samyn, and J. M. Pearson, *Phys. Rev. C* **75**, 064312 (2007)
- [120] R. Rodriguez-Guzman and L. M. Robledo, *Eur. Phys. J. A* **53**, 245 (2017)
- [121] T. Burvenich, M. Bender, J. A. Maruhn, and P.-G. Reinhard, *Phys. Rev. C* **69**, 014307 (2004)
- [122] P.-G. Reinhard and K. Goeke, *Rep. Prog. Phys.* **50**, 1 (1987)
- [123] C. Simenel, *Eur. Phys. J. A* **48**, 152 (2012)
- [124] C. Simenel and A. S. Umar, *Phys. Rev. C* **89**, 031601(R) (2014)
- [125] P. Goddard, P. Stevenson, and A. Rios, *Phys. Rev. C* **93**, 014620 (2016)
- [126] R. W. Hasse, *Rep. Prog. Phys.* **41**, 1027 (1978)
- [127] S. E. Koonin and J. R. Nix, *Phys. Rev. C* **13**, 209 (1976)
- [128] J. Blocki and H. Flocard, *Nucl. Phys. A* **273**, 45 (1976)
- [129] G. Schutte and L. Wilets, *Z. Phys. A* **286**, 313 (1978)
- [130] M. Samyn, S. Goriely, J.M. Pearson, *Nucl. Phys. A* **725**, 69 (2003)
- [131] L. Bonneau, T. Kawano, T. Watanabe, S. Chiba, *Phys. Rev. C* **75**, 054618 (2007)

- [132] M. Mirea, L. Tassan-Got, C. Stephan and C.O. Bacri, Nucl. Phys. A **735**, 21 (2004)
- [133] M. Mirea, L. Tassan-Got, C. Stephan, C.O. Bacri, P. Stoica and R.C. Bobulescu, J. Phys. G **31**, 1165 (2005)
- [134] M. Mirea, L. Tassan-Got, C. Stephan, C.O. Bacri and R.C. Bobulescu, Phys. Rev. C **76**, 064608 (2007)
- [135] M. Mirea, and R.C. Bobulescu, J. Phys. G **37**, 055106 (2010)
- [136] M. Mirea, Phys. Rev. C **83**, 054608 (2011).
- [137] M. Mirea Phys. Lett. B **717**, 252 (2012)
- [138] M. Mirea, Int. J. Mod. Phys. E **21**, 1250035 (2012)
- [139] M. Mirea, Phys. Rev. C **89**, 034623 (2014)
- [140] M. Mirea, Phys. Rev. C **100**, 014607 (2019)
- [141] M. Mirea, Phys. Rev. C **78**, 044618 (2008)
- [142] L. Landau, Physik. Z. Sowjet. **2**, 46 (1932)
- [143] C. Zener, R. Soc. Lond. **137**, 696702 (1932)
- [144] W. Greiner, J. Y. Park, and W. Scheid, Nuclear molecules. Singapore: World Scientific Publishing, 1995
- [145] A. Bohr and B. R. Mottelson, Nuclear structure Volume II: Nuclear deformations. Singapore: World Scientific Publishing, 1998
- [146] S. E. Koonin and J. R. Nix, Phys. Rev. C **13**, 209228 (1976)
- [147] J. Blocki and H. Flocard, Nucl. Phys. A **273**, 4560 (1976)
- [148] U. Brosa, S. Grossman, A. Muller, Phys. Rep. **197**, 167 (1990)
- [149] M. Mirea, J. Phys. G **43**, 105103 (2016).
- [150] J. R. Nix, Annu. Rev. Nucl. Sci. **22**, 65 (1972)
- [151] H. C. Pauli, Phys. Rep. **7**, 35 (1973)
- [152] K. T. R. Davies and J. R. Nix, Phys. Rev. C **14**, 1977 (1976)
- [153] P. Moller, J. R. Nix, W. D. Myer, and W. J. Swiatecki, At. Data. Nucl. Data. Tables **59**, 185 (1995)

- [154] M. Mirea, O. Bajeat, F. Clapier, F. Ibrahim, A. C. Mueller, N. Pauwels, and J. Proust, *Eur. Phys. J. A* **11**, 59 (2001)
- [155] V. M. Strutinsky, *Nucl. Phys. A* **95**, 420 (1967)
- [156] M. Mirea, D.S. Delion, and A. Sandulescu, *Proc. Romanian Acad. A* **18**, 50 (2017).
- [157] M. Mirea, *Phys. Rev. C* **89**, 034623 (2014)
- [158] A. Sandulescu and M. Mirea, *Eur. Phys. J. A* **50**, 110 (2014).
- [159] M. Mirea and A. Sandulescu, *Rom. Rep. Phys.* **70**, 201 (2018)
- [160] A. Sandulescu, M. Mirea and D.S. Delion, *EPL* **101**, 62001 (2013)
- [161] M. Mirea, A. Sandulescu, and D.S. Delion, *Eur. Phys. J. A* **48**, 86 (2012)
- [162] M. Mirea, A. Sandulescu, and D.S. Delion, *Nucl. Phys. A* **870-871**, 23 (2011)
- [163] M. Mirea, R. Budaca, and A. Sandulescu, *Ann. Phys* **380**, 154 (2017)
- [164] K.H. Schmidt and B. Jurado, *Phys. Rev. C* **83**, 061601(R) (2011)
- [165] W. N. Reisdorf, J. P. Unik, and L. E. Glendenin, *Nucl. Phys. A* **205**, 348 (1973)
- [166] H. Wohlfarth, W. Lang, H.-G. Clerc, H. Schrader, K.-H. Schmidt, and H. Dann, *Phys. Lett. B* **63**, 275 (1976)
- [167] C. Signarbieux, M. Montoya, M. Ribrag, C. Mazur, C. Guet, P. Perrin, and M. Maurel, *J. Phys. Lett.* **42**, 437 (1981)
- [168] E. Schwab, H.-G. Clerc, M. Mutterer, J. P. Theobald, and H. Faust, *Nucl. Phys. A* **577**, 674 (1994).
- [169] F.-J. Hamsch, H.-H. Knitter, and C. Budtz-Jorgensen, *Nucl. Phys. A* **554**, 209 (1993)
- [170] H.-H. Knitter, F.-J. Hamsch, and C. Budtz-Jorgensen, *Nucl. Phys. A* **536**, 221 (1992)
- [171] F. Rejmund, A. V. Ignatyuk, A. R. Junghans, and K.-H. Schmidt, *Nucl Phys. A* **678**, 215 (2000)
- [172] V. Avrigeanu, A. Florescu, A. Sandulescu, and W. Greiner, *Phys. Rev. C* **52**, R1755 (1995)
- [173] M. Montoya, *J. Phys.* **44**, 785 (1983)

- [174] H.-G. Clerc, in *Heavy Elements and Related New Phenomena*, edited by W. Greiner and R. K. Gupta (World Scientific, Singapore, 1999), p. 471
- [175] M. Caamano, F. Rejmund, and K.-H. Schmidt, *J. Phys. G* **38**, 035101 (2011)
- [176] B. Jurado and K.-H. Schmidt, *EPJ Web of Conferences* **62**, 07003 (2013)
- [177] P. Armbruster, in *Proceedings of the International Workshop Gross Properties of Nuclei and Nuclear Excitations III*, edited by W. J. Myers (Kleinwalsertal, Austria, 1975), p. 32, Technische Hochschule Darmstadt AED-Conf-75-009-000
- [178] H. Nifenecker, C. Signarbieux, R. Babinet, and J. Poitou, in *Proceedings of the Third IAEA Symposium on the Physics and Chemistry of Fission*, Rochester, NY, August 13-17, 1973, Vol. 2 (International Atomic Energy Agency, Vienna, 1974), p. 117
- [179] J.A. Wheeler, *Niels Bohr and the Development of Physics*, edited by W. Pauli, L. Rosenfeld, and W. Weisskopf (Pergamon Press, London, 1955) p. 163
- [180] C.E. Till, *Review of Modern Physics* **71**, S451 (1999)
- [181] "European Roadmap for Developing Accelerator Driven Systems (ADS) for nuclear waste transmutations (April 2001)"